

# How Do Organic Batteries Work? Theoretical and Design Principles of Electrode Materials for All-Organic Batteries

Robin Wessling, Philipp Penert, and Birgit Esser\*

Post-Li battery technologies are becoming increasingly important. The diverse range of electrically powered devices requires a diversification of electrochemical energy storage technologies. Organic electrode materials are of particular importance for alternative batteries, not only because of the natural abundance of their constituting elements and low toxicity, but also because of the operating principle of their redox reactions and their compatibility with many types of battery chemistries, including multivalent metal and anionic batteries. All-organic batteries are a still a “young” field of research but offer promising opportunities in terms of mechanical and processing properties. In the development of batteries using organic electrode materials the understanding of their redox mechanisms, of the different cell types and the correct interpretation of data is of utmost importance. This comprehensive review offers insight into the working principle of organic-based batteries, into material design considerations, structure-property relations, highlighting the importance of standardized terminology, and into the characterization of newly developed organic electrode materials in battery cells, distinguishing between half-cells and full-cells.

efficiently storing electrical energy and releasing it again when required: Storage in electrical form in capacitors or supercapacitors, or conversion to electrochemical potential in rechargeable batteries. While capacitors can absorb and release energy quickly (high power), batteries generally offer a higher and more stable potential with much larger capacity (high energy), which is advantageous for most applications, especially for powering electrical devices.

Battery-based electrochemical energy storage involves the basic concept of faradaic processes within an electrode. In the inorganic materials commonly used today, this is achieved by changing the oxidation state of a (transition) metal, which changes its electrochemical potential, thereby storing (or releasing) energy. For this process, one or more counterions must penetrate a crystal structure by insertion or intercalation,

hence the name insertion materials. After the emergence of this technology in the 1960s to 1970s,<sup>[2,3]</sup> great efforts were directed at understanding and optimizing these systems, which led to metal ion-based batteries becoming the leading technology in all areas of application today.<sup>[3]</sup> Lithium-ion batteries (LIBs) occupy a special position within this group as the fastest-growing and predominant technology today.

LIBs, which are based on inorganic materials, such as nickel-manganese cobalt oxides (NMC) or the increasingly emerging lithium-iron phosphates, currently account for the majority of produced annually battery capacity.<sup>[4]</sup> However, following a steady decline in price per kWh due to improved manufacturing methods and system efficiencies, the manufacturing cost of LIBs increased for the first time in history from 2021 to 2022.<sup>[5–7]</sup> This was a direct result of the price of key resources, such as lithium and nickel, sharply rising due to supply constraints and the still significant underutilization of recycling of battery electrode materials.<sup>[5–7]</sup> This circumstance marks a key turning point for the trajectory of the rechargeable battery market, as forecasts for global lithium demand now exceed that of global lithium production by 2030.<sup>[8,9]</sup>

This aspect and the potential for conflict due to the inhomogeneous geographical distribution of natural nickel<sup>[10,11]</sup> and cobalt deposits<sup>[12–14]</sup> are among the biggest issues with the LIB technology. For this reason, increasing efforts are directed towards the development of alternative battery technologies and materials

## 1. Introduction

### 1.1. Motivation

Electrochemical energy storage has developed into a technology that is an integral part of today's world. From mobile applications to the steadily growing electric vehicle sector and stationary storage in the grid sector, the demand for reliable energy storage is constantly increasing.<sup>[1]</sup> Two different technologies exist for

R. Wessling<sup>[+]</sup>, P. Penert, B. Esser  
Institute of Organic Chemistry II and Advanced Materials  
Ulm University  
Albert-Einstein-Allee 11, 89081 Ulm, Germany  
E-mail: [birgit.esser@uni-ulm.de](mailto:birgit.esser@uni-ulm.de)

 The ORCID identification number(s) for the author(s) of this article can be found under <https://doi.org/10.1002/aenm.202500150>

[+]Present address: Department of Energy Conversion and Storage, Technical University of Denmark, Fysikvej, Building 310, Kgs. Lyngby 2800, Denmark

© 2025 The Author(s). Advanced Energy Materials published by Wiley-VCH GmbH. This is an open access article under the terms of the [Creative Commons Attribution](#) License, which permits use, distribution and reproduction in any medium, provided the original work is properly cited.

DOI: 10.1002/aenm.202500150

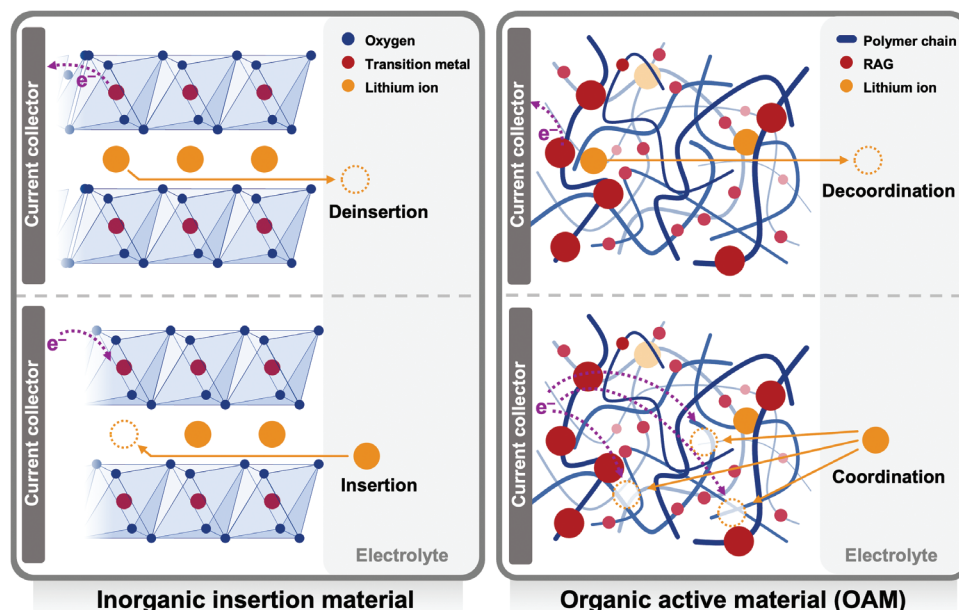


**Figure 1.** Schematic comparison of crystalline inorganic insertion materials with OAMs (represented by an amorphous redox polymer). **Left:** (De)insertion of lithium ions into the crystal lattice of an  $\text{LiMO}_2$ -like crystal structure with fixed positions for the lithium ions. **Right:** (De)coordination of lithium ions by n-type redox-active groups (RAGs) upon their (oxidation) reduction in an amorphous OAM.

that are independent of lithium and (transition) metals as resources.<sup>[15]</sup> Some inorganic-based approaches, such as the so-called post-lithium-metal-ion,<sup>[16–18]</sup> metal-sulfur<sup>[19–21]</sup> and metal-air<sup>[22,23]</sup> batteries, have slowly emerged in recent decades. However, these alternatives struggle with other difficulties, such as slow kinetics, lower working potential, low mobile applicability, or even greater safety concerns than the technologies they are intended to replace.

A far more revolutionary approach is to completely abandon the use of metals as a redox centers for storing electrons. Organic materials are promising candidates for this alternative. They consist of elements that are available in large quantities, such as carbon, hydrogen, oxygen, nitrogen, and sulfur. This eliminates the problem of geographical dependence on raw material reserves. This advantage of sustainability is complemented by mechanistic effects.

## 1.2. Background and Concepts

The redox activity of organic electrode-active materials (OAMs) is based on rearrangements of covalent bonds and/or the redistribution of delocalized electrons during the redox reaction. Delocalization changes the oxidation state of an entire group of atoms rather than that of a single metal atom or ion. Since the energy is stored in electron rearrangements of delocalized systems rather than changes in a crystal structure, the reorganization energy of the respective electron-transfer reaction is usually much lower in organic than in inorganic materials. More importantly, the charges in the respective materials need to be balanced by ions. These ions (i.e., lithium ions) move much more slowly through a highly ordered crystal structure than through an amorphous organic material. **Figure 1** shows a schematic comparison of the

ion pathway in an insertion material, exemplified by an  $\text{LiMO}_2$  structure, and an amorphous redox polymer as OAM. In the latter (red) redox-active groups (RAGs; in this case of n-type) are located on (blue) polymer chains. The amorphous structure can enable much faster kinetics and therefore higher charge and discharge rates for OAM-based electrodes.<sup>[24,25]</sup>

Apart from these faster ion-diffusion kinetics, the amorphous structure of many OAMs allows the production of flexible and/or transparent electrodes and batteries.<sup>[26]</sup> This makes organic batteries particularly interesting for non-conventional applications with specific requirements that inorganic materials cannot fulfill. Reported examples of such devices include flexible, stretchable, or bendable batteries<sup>[27–31]</sup> for wearable electronics, printable batteries,<sup>[32,33]</sup> edible batteries,<sup>[34]</sup> and photo-batteries.<sup>[35,36]</sup>

Arguably the most important advantage of OAMs is their structural and chemical variability and versatility. The modular, building-block nature of organic chemistry and the capabilities of organic synthesis are its greatest strength. The redox activity of organic molecules is based on much more discrete subunits and functional groups than the more global crystal structures of inorganic materials. The synthetic accessibility of these subunits is defined by stepwise routes that provide ample room for almost endless design possibilities and divergent synthesis. In addition, the structure-property relationships of organic molecules have been studied in detail, allowing intelligent design of organic structures with tailored properties for the desired application.<sup>[37–39]</sup>

Modern theoretical chemistry, in particular density functional theory (DFT), plays an important role in the design and development of organic functional materials.<sup>[40,41]</sup> In addition, artificial intelligence (AI) and machine learning (ML) have been introduced into this process, opening up groundbreaking new possibilities for screening (sub)structures based on empirical data.

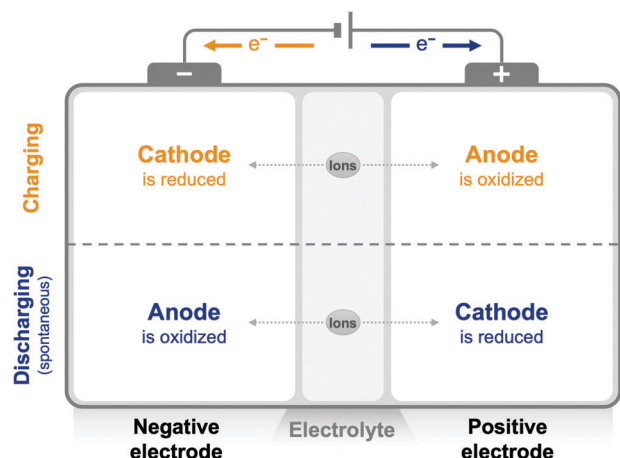


**Figure 2.** Schematic illustration of the working principle of a battery cell with nomenclature as anode or cathode during discharging and charging. The polarity (positive and negative) of the battery is invariant. For the sake of simplicity, the role of the electrolyte is reduced to a migrating ion. Ionic mechanisms will be discussed in more detail later on.

It is predicted that the impact of AI and ML will immensely increase in the near future.<sup>[42–45]</sup> For battery materials, Carvalho et al. made a major breakthrough in 2022 when they implemented DFT-enhanced AI to automatically screen 20 million molecules from databases. Their model was then able to identify 459 promising molecules.<sup>[46]</sup> Approaches like these will dramatically facilitate material design in the future.

## 2. Battery-Cell Mechanisms

The basis of a battery is one or more so-called electrochemical cells, which consist of two electrodes connected by an ion-conducting (but electrically insulating) electrolyte (Figure 2). One electrode acts as the positive (+) pole (or terminal) and the other as the negative (–) pole. To operate the cell in either charge or discharge mode, the terminals are connected to a voltage source or load, respectively. When charging, the active material at the positive electrode is oxidized, i.e., electrons are removed and transported to the negative electrode via the external circuit (orange arrow in Figure 2). When discharging, the electrons are returned to the positive electrode, which leads to the reduction of the active material (blue arrow in Figure 2). The positive electrode always contains the material with the more positive absolute redox potential. Opposite to the positive electrode is the negative electrode. Here, the active material is reduced during charging and oxidized during discharging. Depending on the direction of the current (i.e., whether the cell is being charged or discharged), the roles of cathode and anode are swapped between the electrodes, while the assignment of the poles is invariant during operation and is the most unambiguous way of referring to the respective electrodes. When charging, the negative electrode acts as the cathode, and the positive electrode as the anode. This is reversed when discharging. Herein, we will adhere to this general (and physically more correct) nomenclature. It is, however, worth noting that in the literature, an alternative naming convention has prevailed, in which the positive electrode is called the cathode and the negative is called the anode. Based on their respective

role during the discharging process (e.g., the spontaneous process;  $\Delta G < 0$ ).

### 2.1. Electrochemical Half-Cell Energetics

Regardless of the active materials used, an electrochemical cell can be divided into two subsystems. As the name suggests, every redox reaction consists of a reagent that is reduced and one that is oxidized. In an electrochemical cell, these processes are spatially separated into the two electrodes. Each electrode material in contact with the electrolyte defines an electrochemical half-cell (EHC).

An example system could consist of two OAM redox pairs  $A/A^+$  (molecule A, blue in Figure 3) and  $B/B^+$  (molecule B, red), assuming p-type redox activity (see Figure 9 for types of organic redox-active groups). Each of the pairs forms an independent EHC ( $EHC_A$  and  $EHC_B$ ).  $B/B^+$  has a higher redox potential than  $A/A^+$ , making  $A/A^+$  the negative and  $B/B^+$  the positive electrode, as shown in the exemplary cyclic voltammograms (CVs) of A and B in Figure 3a. The corresponding redox reactions for the resulting battery cell with  $A/A^+$  as negative and  $B/B^+$  as positive electrode are also shown in Figure 3b.

The functionality of two redox pairs is determined solely by their relative redox potentials. The EHC with the higher potential is always the positive electrode and the one with the lower potential is the negative electrode. In general, functional EHCs can theoretically be combined in batteries in any combination. For example, if B is replaced by another p-type material C ( $C/C^+$ , yellow in Figure 3), A would still function as negative electrode as long as the redox potential of C is higher than that of A. The chemistry of each of the redox pairs in the EHCs is independent of that of the other. For  $EHC_A$ , it does not matter where the electron from the oxidation of A goes as long as  $A^+$  is stable after the reaction. The same applies to reductions in n-type materials.

This separability of batteries into two EHCs and the resulting combinability of any two EHCs is exploited in the development of organic active battery materials. If two new materials with unknown properties were tested directly against each other in a battery, it would not be possible to determine, which material is responsible for different aspects of the measured electrochemical behavior of this cell. Therefore, to investigate only the one reaction of interest, a special cell setup can be used, in which only the potential of one EHC is effectively investigated, even though the battery consists of two EHCs. This is achieved by using one of the two EHCs in a large stoichiometric excess compared to the EHC of interest. This cell setup is called a half-cell because it allows studying only one of the EHCs, which represents half of a battery. It is important to note that the term half-cell regularly leads to confusion, as a half-cell battery still consists of two EHCs.

If the EHC  $B/B^+$  is to be investigated in a half-cell setup, both the negative electrode material A and its other redox form  $A^+$  are supplied in large excess compared to the amount of  $B/B^+$ . The potential of the positive electrode (B) then changes according to its state of charge (SOC). However, the large surplus of A and  $A^+$  acts as an electrochemical buffer (compare acid-base buffer). The comparatively small amount of charge required to change the SOC of the positive electrode does not lead to a significant change in the SOC of the negative electrode due to its

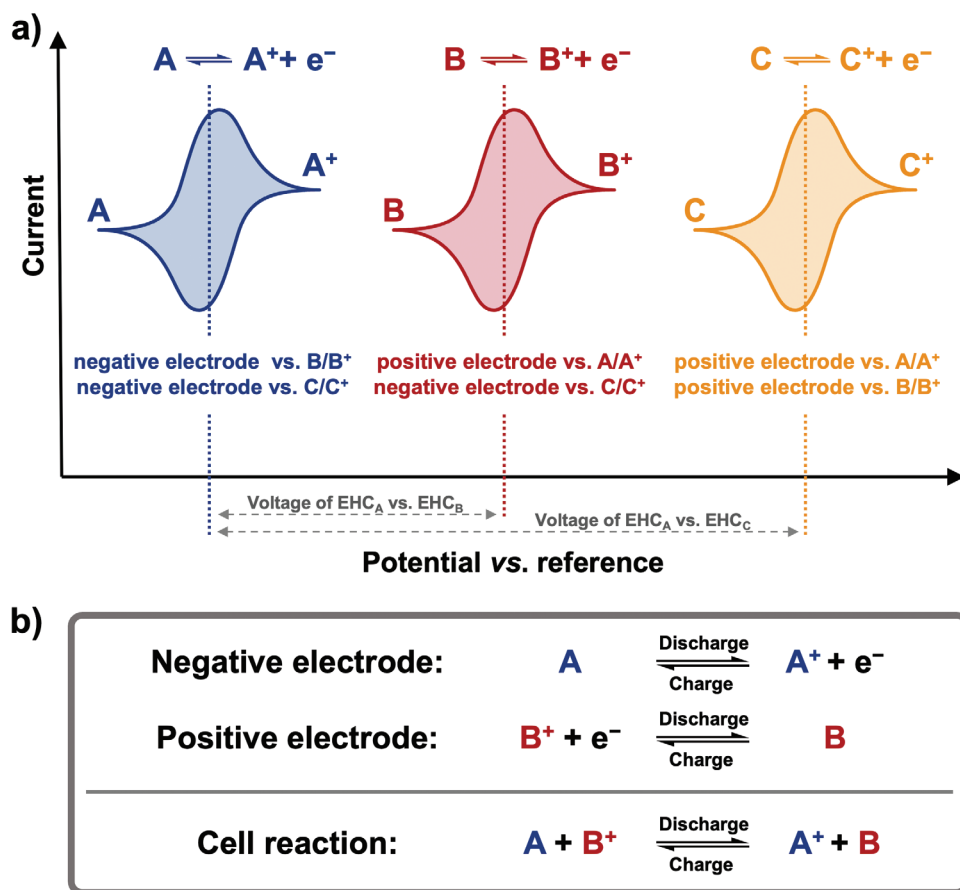


**Figure 3.** a) Schematic representation of the cyclic voltammograms of three exemplary p-type redox couples A, B, and C. Each is capable of one reversible oxidation, but the couples have different redox-potentials ( $E_{1/2}$ ). Any two of them can be coupled with each other. A, with the lowest  $E_{1/2}$ , will always be the negative electrode, while C will always be the positive electrode. B changes its role with respect to the coupled redox pair. b) Exemplary redox reaction of battery consisting of  $\text{EHC}_A$  and  $\text{EHC}_B$ .

much larger capacity. In this way, the voltage of the entire cell within the capacity window of the positive electrode is only dependent on the potential of the same electrode.

For a better understanding of this principle, it may be explained using two vase-like liquid containers, as schematically shown in **Figure 4a**. Each electrode/EHC is represented by a vase.

As the negative electrode  $A/A^+$  (blue) is supplied in large quantity, the left vase has a large volume. The contained liquid is the amount of oxidized species  $A^+$ , and the remaining empty volume represents the amount of neutral species A still to be oxidized. The same holds for the smaller vase with B and  $B^+$  (red). The total volume of the vases thus symbolizes the capacity of the respective EHC. The height of the liquid level in the containers represents the electrochemical potential. The difference in height between the liquid levels of the respective vessels therefore corresponds to the voltage of the battery ( $V_{\text{half/full-cell}}$ ).

The faradaic character of the charging/discharging processes of the EHCs is indicated by the non-tubular shape of the vases (**Figure 5**): The filling height does not increase linearly with the amount of liquid that is added, as would be expected for an ideal capacitor. Instead, when filling the empty container, the liquid level first rises linearly while the level is still within the tubular region of the vase (outside the redox-active potential window of

the respective reaction). Then, as soon as the level reaches the bulb of the vase (onset potential of the redox-reaction), more and more liquid is required to increase the liquid level (charges that are added to the EHC now react in the redox-reaction rather than building up potential). After the bulb is completely filled (the capacity of the redox-reaction is exhausted) the filling level reverts to being linearly dependent on the volume added. The top and bottom of the vases correspond to the potential-stability limits of the EHC. **Figure 5** depicts how the cyclic voltammogram of a redox-couple  $B/B^+$  translates into a charge curve during constant current (galvanostatic) charging (filling of the vase).

In a half-cell (significantly different vessel sizes; **Figure 4a**), the transfer of the liquid volume (charge) from one vessel to another (charging/discharging) leads to a negligible change in the liquid level in the large vessel, but to a significant change in the small vessel. Therefore, the change in battery voltage ( $\Delta V_{\text{half-cell}}$ ) is only defined by the change in positive-electrode potential ( $\Delta E_{\text{pos. electrode}}$ ).

Consequently, the transfer of liquid reveals information about the small vase, while the large vase only serves as a reservoir. The large electrode (vase) is usually realized by using a surplus of a metal, such as lithium, and a similar excess of electrolyte, containing the corresponding metal ions in large numbers.<sup>[47]</sup>



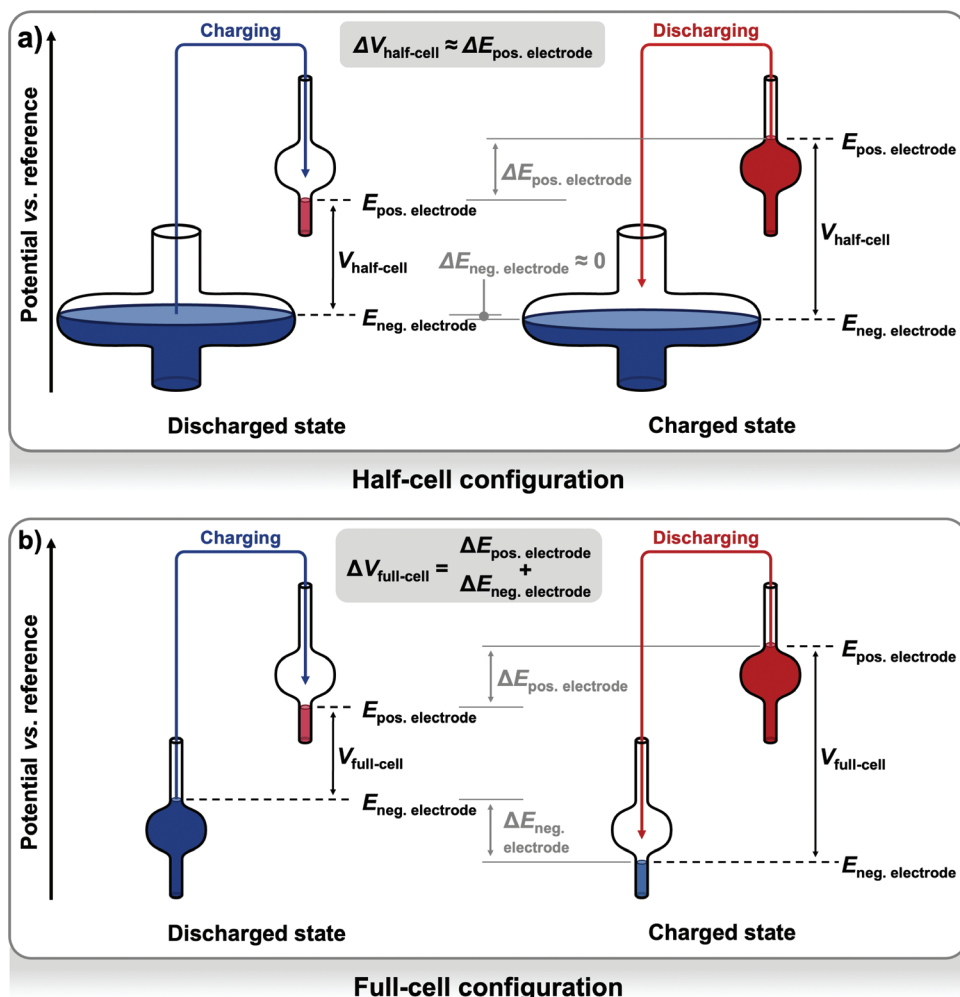


**Figure 4.** Schematic of the capacities of a half-cell (a) and full-cell configuration (b) with the electrodes represented as vases. Level of the liquid  $\hat{=}$  potential of the electrode, volume of the liquid  $\hat{=}$  charge, volume of an entire vase  $\hat{=}$  capacity of the electrode, transferred liquid during charging/discharging  $\hat{=}$  capacity of the battery systems in a set potential window, transfer of liquid from the lower to the higher vase  $\hat{=}$  charging, transfer of liquid from the higher to the lower vase  $\hat{=}$  discharging.

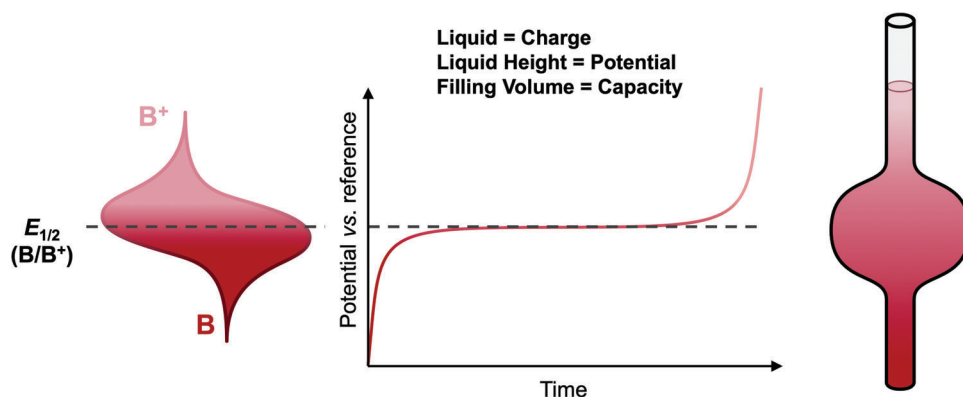


**Figure 5.** Schematic showing the analogy of the vase-like container (in shape) to the CV curve of the redox couple  $B/B^+$ .

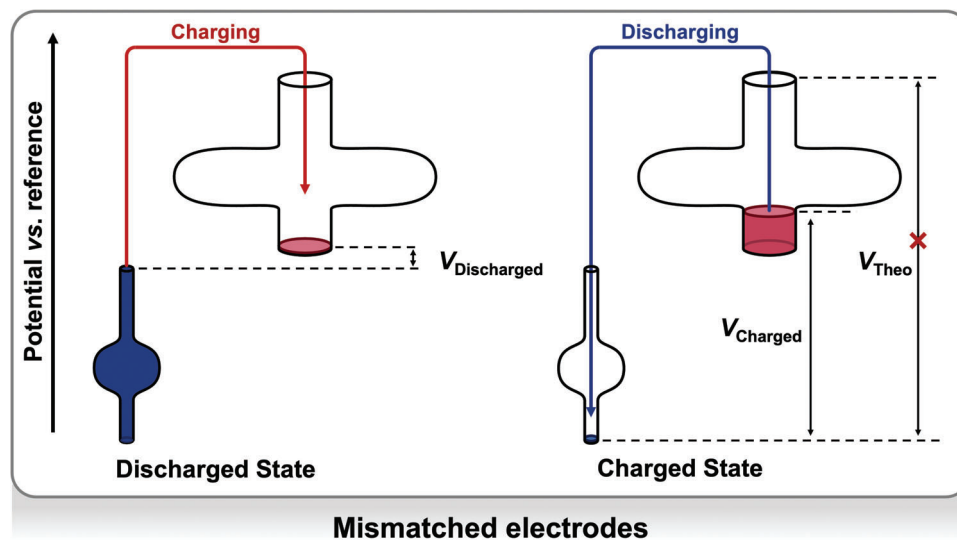


**Figure 6.** Effects of misbalancing the capacity of a full-cell battery. The theoretical voltage difference between the empty negative electrode and the full positive electrode can never be reached, since the capacity of the former is insufficient to fill the latter. If the charging device is configured to reach a certain voltage to conclude the charge, the negative electrode will be deep-discharged in an attempt to extract more charge. While the positive electrode is capable of being charged further, this may irreversibly damage the negative electrode as this would mean an operation outside its stable potential window.

Thus, both the reduced (metal) and the oxidized (ion) form of the metal/metal<sup>+</sup> redox couple are present in large amounts compared to the analyte molecule.

## 2.2. Full-Cell Reactions

To ensure easy comparability, the same redox process is shown in Figure 4b for the case of a full-cell, in which both vases are of the same size. It is obvious that for the full-cell, the change in battery voltage ( $\Delta V_{\text{half-cell}}$ ) is the sum of the changes in the two electrode potentials ( $\Delta E_{\text{pos. electrode}} + \Delta E_{\text{neg. electrode}}$ ).

It should be noted that – although practically any two EHCs can be combined to form a battery – in reality a full-cell will always differ slightly from a combination of the two EHCs tested in half-cells and will require additional optimization. While thermodynamic properties, such as the redox potential, can be investigated in detail in half-cells, the kinetics of the corresponding full-cell can at best be estimated. The kinetics are always based on the performance of both electrodes. So, even if both EHCs were optimized compared to the same reference EHC, the latter will likely have influenced the kinetics in both characterizations.

A half-cell would never be commercially viable, as the large excess on one side represents a waste of material, volume, and mass. For this reason, half-cell batteries are only used in research and development. In contrast, a full-cell battery is a design with equal (or nearly equal) capacities in both EHCs. The development and manufacturing of full-cells is a much more complicated process, as the two EHCs must be balanced in terms of capacity, and both must be compatible with all other components of the system. Even if two fully functional EHCs are available, combining them into a functioning full-cell requires significant optimization. An incorrect balance can lead to undesirable potential curves during cycling, to overpotentials, and thus to decomposi-

tion. If one of the electrodes unintentionally has a larger capacity than the other, this can lead to a deep discharge or overcharging of the EHC with a lower capacity, as the voltage limits are not observed. This effect is shown schematically in Figure 6.

## 2.3. Rate Dependence of Battery Capacity

The vase-analogy can also be expanded from the above-mentioned “thermodynamic” considerations to the kinetics of a battery system. One of the main issues of batteries is the rate at which the system may be charged and discharged. This rate is mainly dependent on the diffusion of charge carriers inside the battery, which may be visualized as the viscosity of the fluid being filled into the vases. Low-viscosity fluids like water (EHC with high charge carrier mobility/diffusivity) fill up the volume of the vase quickly and uniformly. This results in a situation, in which the full volume of the vase will always be used when filling it to the top. On the other hand, a liquid with high viscosity like honey (EHC with low charge carrier mobility/diffusivity) will limit the flow through the narrow opening of the vase. For high filling rates, this can result in a situation in which the narrow tubular opening is filled more quickly than the liquid can pass on into the bulb of the vase, which essentially “clogs” it. In this case, the liquid level in the vase will reach the top before the full volume of the vase is actually filled.

This case is always true in real batteries. At very high charge/discharge rates (strongly dependent on the cell chemistry and electrode structure), the charge carriers moving into the system at the interface of electrode and current collector will encounter redox centers that already have undergone the target redox reaction. Hence, in order to use this charge carrier in the redox reaction, it has to diffuse into the bulk of the electrode to find an unreacted center. These diffusion processes are comparably

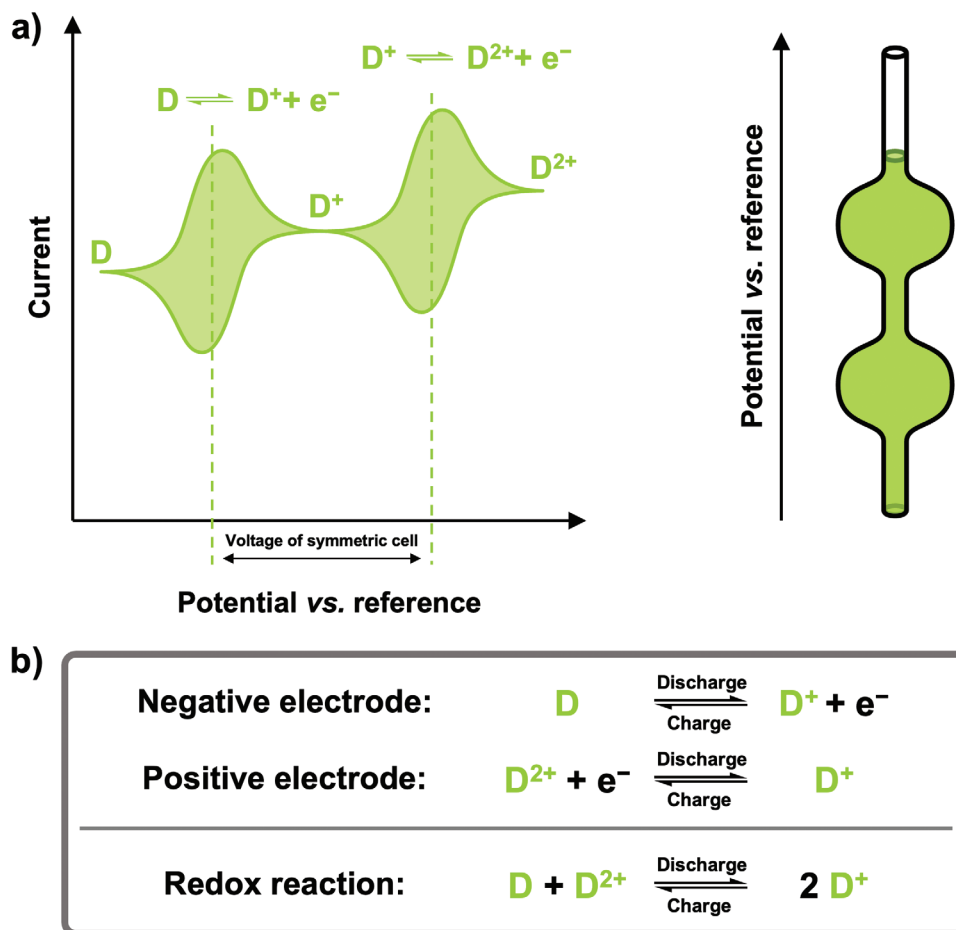


**Figure 7.** a) Schematic representation of the CV of molecule D, which is capable of two oxidations. Coupling two identical electrodes containing this material as anode and cathode results in a symmetrical full-cell. The theoretical voltage of this battery is indicated at the bottom of the CV. On the right is shown a vase-analogy representation of the multi-electron EHC<sub>D</sub>. Each of the two bulges represents one of the redox reactions. The lower one is the process between neutral and cationic state and the upper one is the process between cationic and dicationic state. b): Redox reactions corresponding to the symmetrical full-cell based on the twofold oxidizable D.

slow in solid-state electrodes, leading to a build-up of “unused” charge carriers at the electrode’s surface, which in turn increases the potential of that electrode to above that of the EHC in equilibrium. As a direct result, the usable capacity of battery electrodes is smaller with increasing charge/discharge rates, an effect described by PEUKERT’S Law.<sup>[48]</sup>

## 2.4. Symmetric Cells

A full-cell system is always limited by the “slower” EHC in terms of kinetics and the “smaller” EHC in terms of capacity. More importantly, full-cells may require compromises when it comes to battery components that are shared by both EHCs, such as the electrolyte and the separator. The electrolyte, with which one of the EHCs achieves optimal results, is not always the same as for the other EHC.

One way of resolving this issue is the fabrication of a so-called symmetrical full-cell. A symmetrical full-cell contains an active material that is capable of several redox processes (i.e., redox couples D/D<sup>+</sup> and D<sup>+</sup>/D<sup>2+</sup>, **Figure 7**). One redox process can then be used in the negative electrode and the other redox process in

the positive electrode. The discharge can be considered as a disproportionation of the redox unit (discharged form D<sup>+</sup> in both electrodes), while the charging can be associated with a disproportionation (charged forms D and D<sup>2+</sup> in negative and positive electrode, respectively). The corresponding processes for an exemplary multi-electron material D are shown in **Figure 7** analogous to the asymmetric cases discussed above. Symmetrical full-cells can significantly reduce the research effort for optimization and make large-scale production much easier.<sup>[49,50]</sup>

In the context of the vase analogy discussed above, a multi-electron EHC would be represented by a vase with two bulges, as shown in **Figure 7a** (right). Each bulge represents one of the two redox processes.

## 3. Charge Storage Mechanisms in Organic Electrode Materials

### 3.1. Historical Perspective

In order to convert electrical to electrochemical energy, electrons must be released or absorbed by a chemical entity. As already

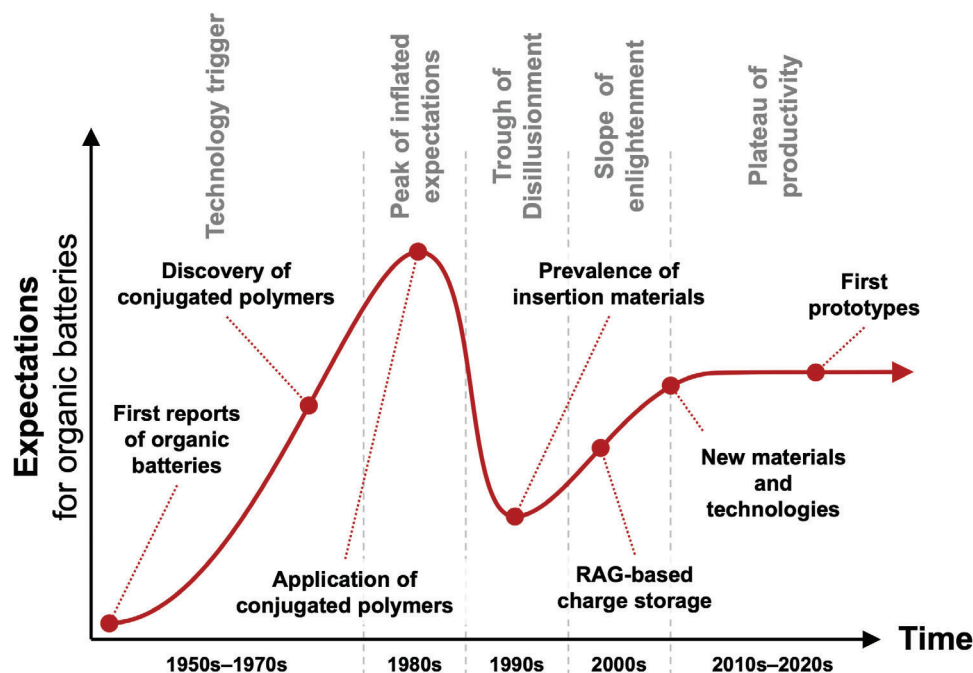


**Figure 8.** Schematic representation of the expectations toward organic battery technology over time. Key events in the development are marked and compared to the stages of a GARTNER-cycle.

mentioned, in inorganic materials this process is based on metals and/or metal ions changing their oxidation state, and ultimately their electrochemical potential. In organic materials, the redox process is based on a change in the oxidation state of a carbon or a heteroatom. These atoms are part of larger molecular entities, and in many cases, resulting charges are delocalized between several atoms.

The first reports on OAMs were made by Morehouse and Glicksman in 1957<sup>[51]</sup> and by Williams et al. in 1969,<sup>[52]</sup> but significant research interest emerged only in the later 20th century with the idea of utilizing the newly discovered class of conjugated polymers. Some of the best-known examples were polyacetylene (1981),<sup>[53]</sup> polyphenylenes (1982),<sup>[54]</sup> polythiophene (1983),<sup>[55]</sup> polyanilines (1984),<sup>[56,57]</sup> and polypyrrole (1986).<sup>[58]</sup> The functional principle was a p- or n-doping of long, linear conjugated polymers during charge or discharge. However, the high delocalization of the charges led to low capacities due to limited maximum doping levels.<sup>[59,60]</sup> Holes (or electrons) stored in conjugated polymer chains would exhibit significant interactions leading to redox potentials that are strongly dependent on the SOC of the material. Following these early systems, OAM-interest waned due to the emergence of a new generation of inorganic insertion materials on both the positive and negative electrode side and the realization that dopant-based conjugated polymers would likely never surpass the capabilities of the then (1987) commercialized lead-acid batteries.<sup>[61]</sup>

A new dawn in the field of energy-storage OAMs began in the early 2000s, when the idea of doping conjugated systems was abandoned and replaced by a new approach of using RAGs, which may or may not be part of larger structures. This approach was only used in a few reports in the first era.<sup>[52,62–64]</sup> RAGs can range from small functional groups (FGs) to larger (but still small

compared to a whole polymer chain) groups. This has the advantage that the redox activity in these subunits is much more localized, which not only potentially reduces molecular weight, but also allows holes or electrons to be stored more independently. In a comparatively short time, a large number of RAGs were identified that can reversibly carry out single or multiple redox reactions. The entire development path of organic batteries can be illustrated abstractly using a GARTNER hype cycle (Figure 8).<sup>[65]</sup>

### 3.2. Classification and Operation of Redox-Active Groups and Stabilization of Charges

Any organic molecule can be oxidized and/or reduced as long as the corresponding driving force for the reaction, the potential difference (voltage), is high enough. So, technically, what makes a molecule an RAG is not its ability to undergo oxidation or reduction, but rather its ability to stabilize the resulting state in the given environment (i.e., in an electrolyte and in the presence of counter ions). This stability is an essential prerequisite for the reversibility of the process to the original state. Only if the process is fully reversible can it also be run cyclically, which of course is the main concern for use in a rechargeable battery.

Although there are RAGs that are based on pure hydrocarbons only,<sup>[66–68]</sup> the origin of the redox activity in most RAGs are heteroatoms, such as oxygen, nitrogen, sulfur, and phosphorus, which are linked to a conjugated  $\pi$ -system. Upon reduction/oxidation of the system, these heteroatoms can accept or donate free electrons from or to the conjugated system through resonance effects, stabilizing the resulting charge. The first to describe this systematically were DEUCHERT and HÜNIG in 1978.<sup>[69]</sup> An adapted version of their systematics is shown in Figure 9. Delocalization not only stabilizes the energy of the orbitals



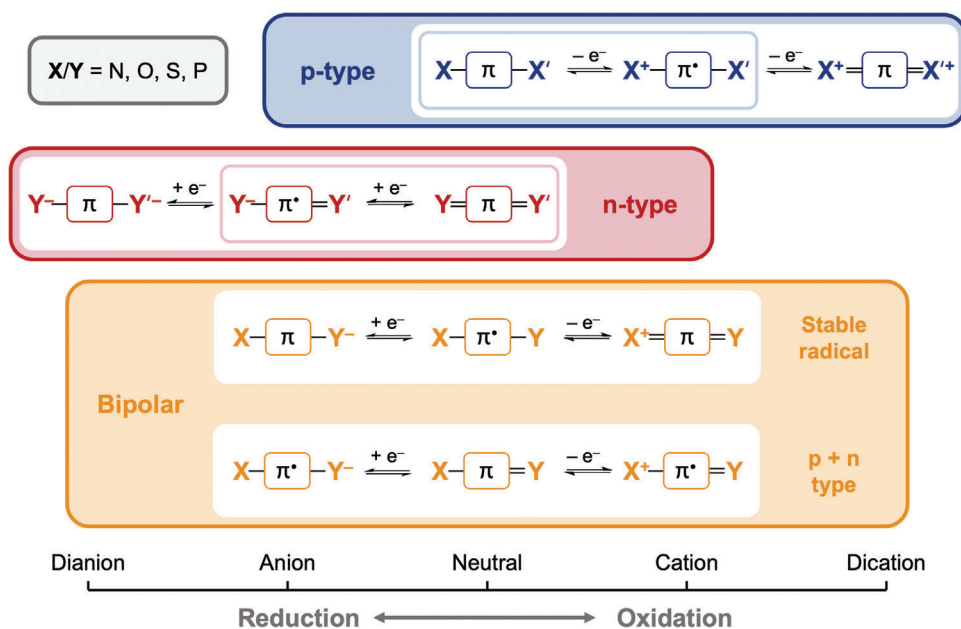


**Figure 9.** Adapted version of DEUCHERT and HÜNIC's classification<sup>[69]</sup> of the three possible polarities p-type, n-type, and bipolar of organic RAGs and their corresponding redox reactions. X/X' and Y/Y' are heteroatoms like N, O, S, or P. Inner boxes in p-type and n-type signify the single-electron process, for which X' = H or Y' = H, respectively. Counterions are omitted for clarity.

involved, but also spatially distributes the charge or spin density, thereby minimizing electrostatic forces.

Another, less common mechanism for charge stabilization is the steric shielding of the charged redox center, a strategy that is mainly used for stable radical RAGs, such as 2,2,6,6-tetramethylpiperidinyloxy (TEMPO)<sup>[70]</sup> (Figure 9).

Stabilization mechanisms prevent undesired secondary reactions of the respective redox process. The possibilities for side reactions are manifold and range from bond cleavage to bond formation (intra- and intermolecular), especially with electrolyte components. In general, all undesirable, activity-changing side reactions are summarized under the term "decomposition."

RAGs can be divided into three different groups, depending on which redox process they are able to stabilize. This classification is derived from DEUCHERT and HÜNIC's considerations.<sup>[69]</sup> So-called p-type RAGs (Figure 9, top) can be oxidized and are able to stabilize a positive charge, while n-type RAGs (Figure 9, middle) can be reduced and can stabilize negative charges. A small number of RAGs are capable of both processes and are therefore referred to as bipolar (Figure 9, bottom). In these definitions, the state in which the respective molecule or RAG is in under ambient conditions is irrelevant for the nomenclature.

In some cases, the definitions are extended to whole molecules or their subunits. A molecular structure that contains both a p-type and an n-type RAG can be considered a bipolar molecule despite the absence of a bipolar RAG, such as a stable radical (Figure 9, below).

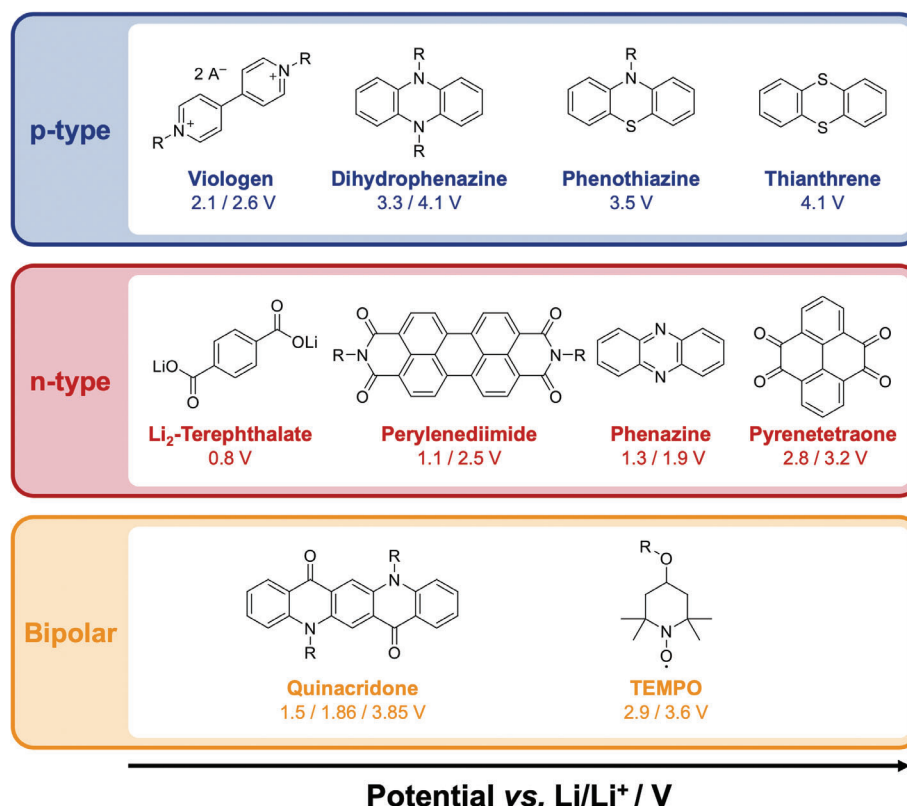
In a RAG, which is generally capable of a stable redox activity, the properties can be tailored by substituting the conjugated system with FGs, for instance, of electron-donating or -withdrawing character.

Figure 10 provides an overview of selected RAGs that have been heavily investigated in recent years.

### 3.3. Operating Mechanisms of All-Organic Batteries

With the introduced RAGs different battery operating mechanisms are possible, where the polarity of the RAGs in each organic material determines how the resulting OAM functions. When a battery is charged or discharged, the resulting charges on the electrodes are balanced by the corresponding ions from the electrolyte in order to reduce the electrostatic charge on the electrodes, which would otherwise inhibit their function. The type of ions required to balance the charges in the negative and positive electrode naturally plays an important role and depends on the polarity of the RAG used for the respective reactions. With two different polarities (n- and p-type) of RAGs, three different configurations are conceivable for the combination of two OAMs (Figure 11). Bipolar RAGs can be used in both roles (n or p) and therefore do not increase the number of possible permutations.

The simplest approach is to combine an n-type OAM as the negative electrode with a p-type OAM as the positive electrode. This usually leads to the highest working potentials of all three options, as n-type OAMs typically have much lower redox potentials than p-type OAMs (Figure 10). Such a combination operates in a dual-ion configuration (Figure 11a). The n-type material at the negative electrode is reduced during charge, while the p-type OAM at the positive electrode is oxidized. Therefore, the overall chemical charge (independent of sign) of the organic molecules increases during the charging process. To balance these charges, cations migrate from the electrolyte to the negative electrode, while anions migrate from the electrolyte to the positive electrode. Therefore, both ions of the electrolyte are involved in the cycle mechanism, which leads to the term dual ion. As both ions are active, they both have a considerable influence on the kinetics of the processes involved. Theoretically, this configuration could be reversed, resulting in an inverted dual-ion



**Figure 10.** Examples of RAGs sorted by their type and in order of ascending potential versus lithium. Multi-electron RAGs are sorted according to their lower redox potential. p-type: viologen (A = Anion),<sup>[71,72]</sup> dihydrophenazine (DHP),<sup>[73–76]</sup> phenothiazine (PT),<sup>[77–79]</sup> thianthrene;<sup>[80–82]</sup> n-type: Li<sub>2</sub>-terephthalate,<sup>[83]</sup> perylenediimide,<sup>[84–86]</sup> phenazine,<sup>[87,88]</sup> pyrenetetrone (PTO);<sup>[72,89]</sup> Bipolar: TEMPO,<sup>[90]</sup> quinacridone.<sup>[91]</sup>

battery, if a p-type OAM with low redox potential was combined with an n-type OAM of high redox potential. While an advantage of the dual-ion configuration can be a high rate capability,<sup>[92]</sup> a disadvantage is that the electrolyte concentration changes during operation, and typically an excess of electrolyte salt is required.<sup>[93]</sup>

The combination of two n-type RAGs (Figure 11b) leads to a so-called cation-rocking-chair configuration. At the negative electrode, the OAM is reduced during charging and requires a cation to shield the resulting charge, while at the positive electrode the OAM is oxidized from the anionic to its neutral form and releases a cation. During discharge, these processes are reversed. Effectively, only the cation participates in the ion diffusion in the electrolyte and “rocks” back and forth between the two electrodes during the cycle, hence the name rocking chair.

Similarly, the combination of two p-type materials creates an analogous system, which is accordingly referred to as an anion-rocking chair (Figure 11c). The p-type OAM at the negative electrode is reduced during charging, while the one at the positive electrode is oxidized. Accordingly, charge equalization is only performed by the anions.

Both rocking-chair configurations have the unique advantage that only one type of ion is responsible for diffusion within the electrolyte. The remaining ion is inactive and only needed to enable the movement of the active ion. Hence, the concentration of electrolyte salt in the electrolyte remains constant during battery operation. This enables new approaches for electrolyte de-

sign and performance optimization, especially in anion-rocking-chair systems. Here, due to its inactivity, the cation no longer needs to be present as a metal ion that can be coordinated to the RAGs. This has resulted in completely metal-free electrolyte systems based on organic cation salts<sup>[94]</sup> or ionic liquid systems.<sup>[95,96]</sup> Table 1 summarizes the key features of the different cell configurations as well as their advantages and disadvantages. It is worth noting that in a generalized form of Figure 11, the oxidation states 0 and + should technically be referred to as  $x$  and  $x+1$ , respectively, since the neutral state is not necessarily part of the cycle of these materials. Multi-electron RAGs, such as viologens (Figure 10), are an example of this. The stability of the two redox processes of viologens is not equal. Therefore, in some applications they are only cycled between the radical cationic and dicationic states and consequently never reduced to the neutral state.<sup>[71]</sup>

### 3.4. Lithium-Organic Half-Cells as Standard Test Cells

To facilitate and accelerate the process of screening new materials, a simple and reproducible reference system is used. This standard system is the organolithium half-cell. Using elemental lithium in a large excess compared to the OAM eliminates many of the difficulties that would be encountered when testing new materials in fullcells, as well as compatibility issues when combining with other organic materials (see vas analogy in Figure 4a). While the ease of processing lithium metal is a more practical

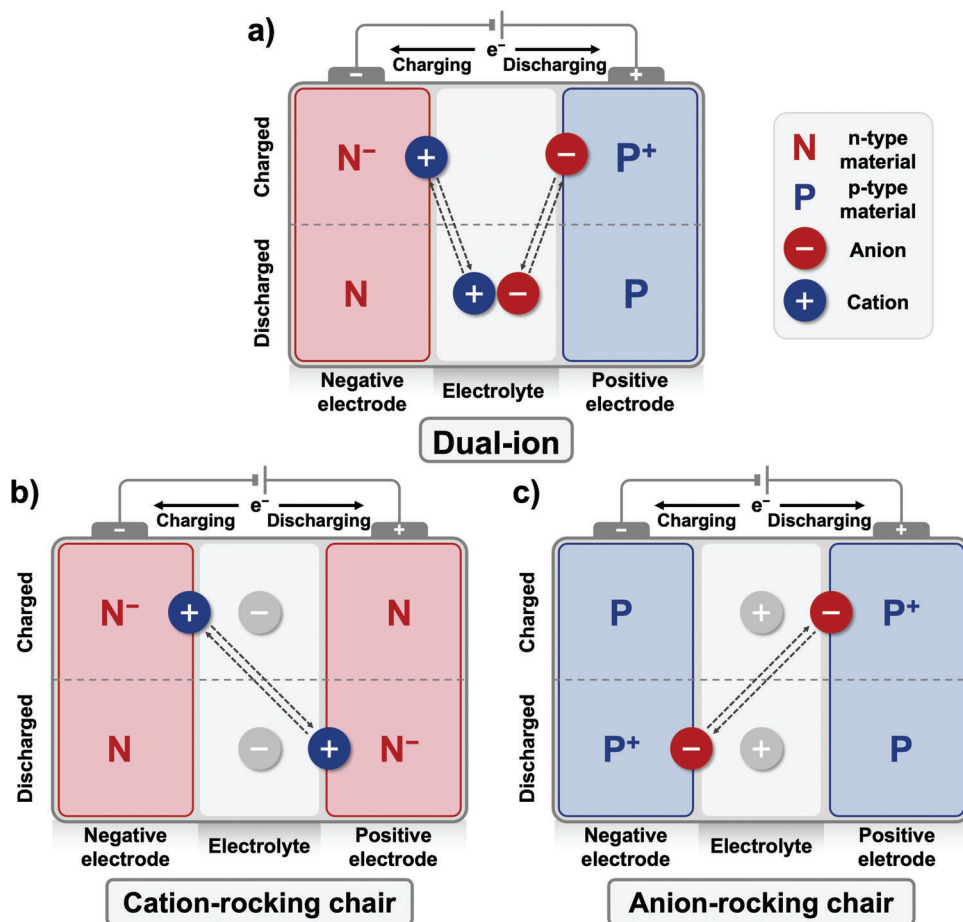


**Figure 11.** Schematic overview of the three main configurations of all-organic batteries and their respective mechanisms. a) Dual-ion configuration, in which both ions are active. They diffuse into the electrodes during charging and back into the electrolyte during discharging. b) Cation-rocking chair configuration and c) anion-rocking chair configuration, in which only the respective ion is active. The inactive ion is grayed out. The active ion moves in between the electrodes during charging and discharging.

**Table 1.** Key features, advantages, and disadvantages of different cell configurations using organic electrode materials.

Cell-type	Key features	Advantages	Disadvantages
Dual-Ion	<ul style="list-style-type: none"> <li>n-type OAM as negative electrode</li> <li>p-type OAM as positive electrode</li> <li>Both anion and cation compensate charges during cell operation</li> </ul>	<ul style="list-style-type: none"> <li>High working potentials</li> </ul>	<ul style="list-style-type: none"> <li>Excess of electrolyte salt needed due to changes in concentration during operation</li> <li>Diffusivity of both ions relevant</li> </ul>
Anion-rocking chair	<ul style="list-style-type: none"> <li>p-type OAMs as negative and positive electrode</li> <li>Anions shuttle to compensate charges</li> </ul>	<ul style="list-style-type: none"> <li>Only one type of ion needs to diffuse through electrolyte, less complex systems</li> <li>No metal cation needed in anion-rocking chair configuration</li> </ul>	<ul style="list-style-type: none"> <li>It is challenging to identify two OAMs of the same polarity with a significant working potential gap in between.</li> </ul>
Cation-rocking chair	<ul style="list-style-type: none"> <li>n-type OAMs as negative and positive electrode</li> <li>Cations shuttle to compensate charges</li> </ul>		

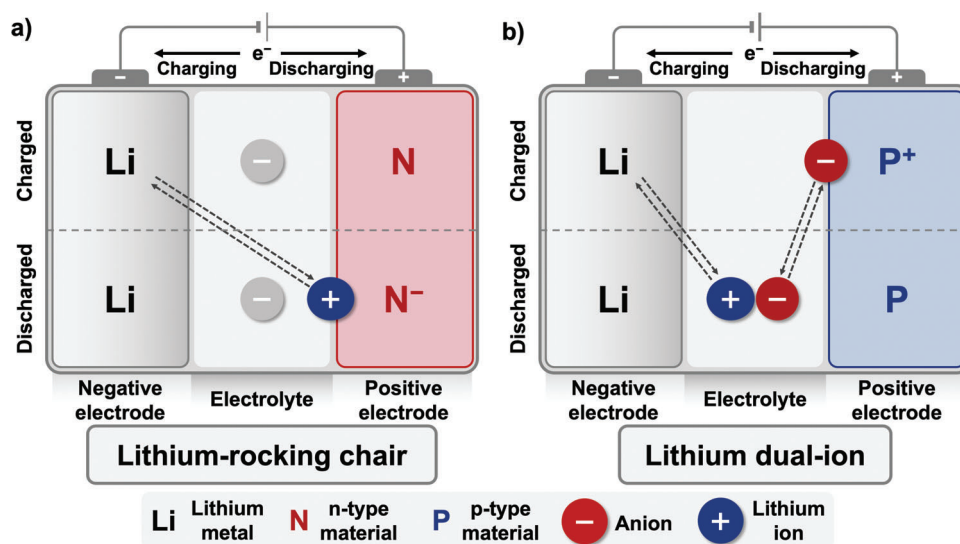


**Figure 12.** Charging and discharging mechanisms of the two configurations of lithium-organic half-cells. a) Lithium-rocking chair pairing lithium metal with an n-type OAM. b) Lithium dual-ion battery pairing lithium metal with a p-type OAM. Mechanisms are analogous to the corresponding full-organic cation-rocking chair and dual-ion configurations when considering the lithium metal negative electrode as substitute for an n-type OAM.

advantage, the use of excess lithium also offers some chemical and physical advantages.

In organic (mostly carbonate-based) electrolytes, a number of standard solvents and salt formulations have been identified that form stable solid-electrolyte interphases (SEIs) on the surface of the lithium metal after comparatively short equilibration times. These layers form in situ at the contact surface of the negative electrode and the electrolyte. Lithium is such a strong reducing agent that the electrolyte begins to decompose as soon as it comes into contact. In the case of an optimized electrolyte, the decomposition products form a stable intermediate layer that is ionically conductive but electrically insulating and protects the negative electrode and electrolyte from further or even unlimited decomposition. The SEI and its positive electrode counterpart, the cathode-electrolyte interphase (CEI), are a very active area of research for inorganic materials, as many researchers believe that a fundamental understanding of the processes during SEI/CEI formation will enable significant improvements for many battery systems.<sup>[97–100]</sup> The ability of lithium to form stable SEIs in a range of optimized electrolytes makes it a reliable option as a negative electrode material in a research context. Many (post-lithium) metals, such as sodium and potassium, are not capable of forming stable SEIs, or the appropriate electrolyte formulations have not yet been discovered. This naturally makes the development of post-lithium battery systems more difficult.<sup>[99]</sup> In addition, the stability of lithium in the electrolyte allows the use of metallic lithium as a reference electrode in a three-electrode arrangement, such as a Swagelok cell. The stability of the redox potential of a lithium reference electrode cannot compete with more complicated reference electrodes, such as partially lithiated lithium-iron phosphate (LiFePO<sub>4</sub>) or lithium titanate (Li<sub>4</sub>Ti<sub>5</sub>O<sub>12</sub>). However, its ease of use makes lithium metal a commonly used option, especially in fundamental research.<sup>[101]</sup>

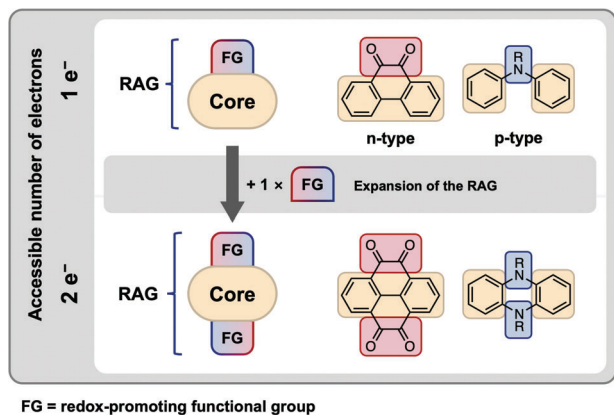
In terms of function and cycling mechanism, a lithium negative electrode can replace the n-type OAM in the setups of

Figure 11, resulting in either a lithium dual-ion system (paired with a p-type OAM) or a lithium rocking-chair system (paired with an n-type OAM). These two configurations are shown in Figure 12 and represent the main types of cells used in the research and development of OAMs. It is important to understand that in Li half-cells, both OAMs intended for use as positive or negative electrode in a later full-cell are tested as positive electrode against lithium due to its low redox potential. This often leads to confusion in the nomenclature of the materials. As the lithium metal and the amount of Li<sup>+</sup>-ions are used in a high excess, one can think of this electrode as the big vase in Figure 4a.

Despite general efforts to develop and commercialize lithium-free and purely organic batteries, most researchers are therefore developing new materials based on lithium half-cells. Only after the investigation of the basic electrochemical properties with regard to lithium will the investigations on more complex systems be continued. There, the material can then be fully characterized and optimized. This approach is possible because organic materials are tolerant to ions of different sizes and charges (Figure 1). OAMs function through the association of counter ions with their charged conjugated systems. Since there is no or little crystalline structure, these associative forces are less influenced by the size or charge of an ion. Due to their structural flexibility, OAMs are adaptable to such changes. This makes organic materials particularly interesting for post-lithium applications and aqueous batteries, as the ionic charges and radii (of the solvation shell) drastically change in these applications.<sup>[24,102]</sup> In contrast, the interlayer distances and ionic forces in crystalline insertion materials are usually too sensitive to ion exchange. Therefore, another ion will likely inhibit the functionality of the material.

## 4. Structural Design of Organic Electrode Materials

Following the mechanistic discussion and functioning of organic batteries, we will now focus on how OAMs have to be designed



**Figure 13.** Schematic representation of two strategies to introduce multi-electron activity to an RAG by adding additional functional groups (FGs).

to work well in battery applications and how synthetic organic chemistry can be applied to tailor the electrochemical properties and improve the material performance.

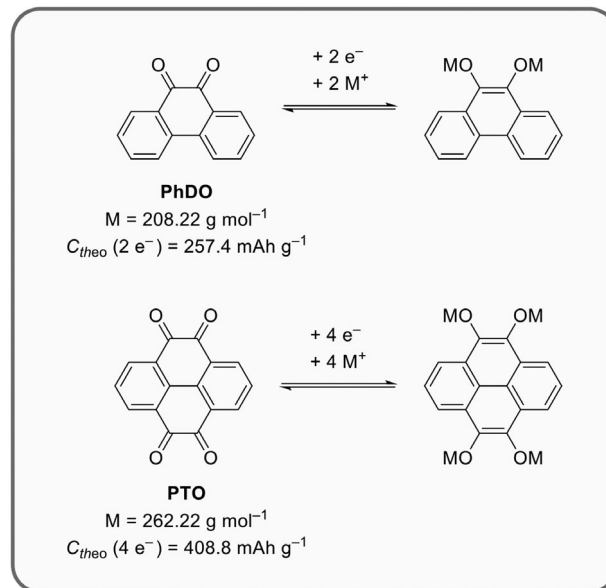
#### 4.1. Enabling Multi-Electron Redox Activity

The theoretical specific capacity  $C_{\text{theo}}$  of organic materials in energy storage applications is limited by their molecular weight, according to Equation (1), where  $n$  is the number of electrons transferred,  $F$  the FARADAY constant and  $M$  is the molecular weight of the molecule or repeating unit.

$$C_{\text{theo}} = \frac{n \cdot F}{M} \quad (1)$$

Consequently, researchers striving for high-capacity materials can pursue two strategies. The first is to minimize molecular weight. This is possible to some extent, but ultimately limited, as many RAGs are based on extended  $\pi$ -systems and contain heteroatoms to stabilize charges. Electrochemically inactive parts of the molecular structure can in some cases be removed by synthetic design. A common example of this is the minimization of solubility-inducing side chains or other motifs that are only important in a preparative context.<sup>[103]</sup> However, this strategy is comparatively ineffective. Doubling the capacity requires halving the molecular weight, which is out of the question for most RAGs. There are special cases where solubility-mediating groups cannot be minimized, but can be thermolytically cleaved off after they have served their purpose within the synthesis route,<sup>[104,105]</sup> but this is only possible for certain systems and cannot be generalized to all chemistries.

The second approach is much more promising, namely to chemically modify the materials in such a way that they enable additional redox activity within the RAG, which leads to an increase in  $n$  in Equation (1). This can be achieved by expanding the RAG by adding redox-active FGs, which is shown schematically in **Figure 13**. This method is only feasible if the additional molecular weight required to introduce an additional redox process does not overcompensate for the capacity gained by the new process.



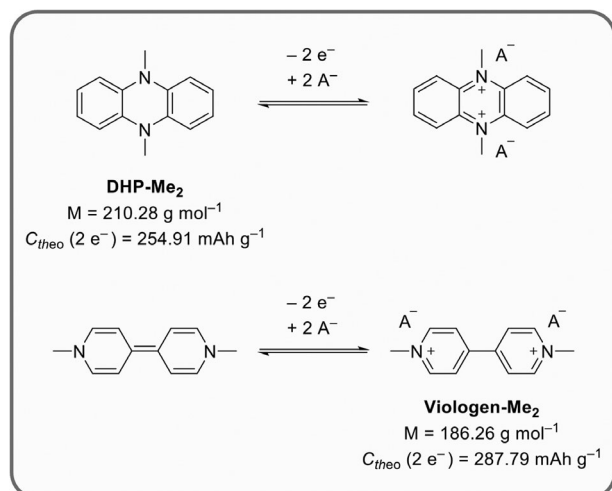
**Scheme 1.** Comparison of the theoretical specific capacity and redox processes of phenanthrene-9,10-dione (PhDO, top) and 4,5,9,10-pyrenetetraone (PTO, bottom).

In n-type materials, a common strategy for the design of multi-electron RAGs is the insertion of additional redox sites in the form of carbonyl FGs into a conjugated system (Figure 13, right).<sup>[59]</sup> An example of this approach would be the change from phenanthrene-9,10-dione (PhDO) to 4,5,9,10-pyrenetetraone (PTO), as shown in Figure 13 and **Scheme 1**. The addition of two carbonyl groups increases the weight by only 26%, but doubles the number of electrons. Overall, this increases the theoretical capacity  $C_{\text{theo}}$  from  $257.4 \text{ mAh g}^{-1}$  ( $2 e^-$ ) to  $408.8 \text{ mAh g}^{-1}$  ( $4 e^-$ ). For PTO, Liang et al. report an observed specific capacity of  $360 \text{ mAh g}^{-1}$  in contrast to  $243 \text{ mAh g}^{-1}$  for PhDO, which is significantly higher and shows the effect of the additional carbonyl groups. A variety of RAGs have been developed based on the carbonyl approach.<sup>[106–110]</sup> Next to the capacity, these structural changes also affect the redox potentials of the RAGs.

In contrast, most p-type RAGs have nitrogen-based redox activity.<sup>[106,109,111–113]</sup> With five valence electrons, nitrogen is not able to form bonds with only one other atom, as oxygen does in carbonyls. In other words, the design options for adding further p-type heteroatoms are different from those of adding more carbonyl moieties. The vast majority of p-type RAGs described in the literature uses nitrogen in N-heterocyclic aromatic compounds or in N-arylated compounds. Simpler N-containing FGs, such as  $-NH_2$  or  $-NMe_2$ , do not provide sufficient charge stabilization, which is why they are rarely found in reports on p-type battery materials. An example for doubling the amount of reversibly accessible oxidation states is by extending a bi- or triarylamine to a 5,10-dihydrophenazine (DHP), as shown in Figure 13 and **Scheme 2** (top). DHP shows a reversible two-electron oxidation, as do many viologens (Scheme 2, bottom).<sup>[71,72,74,76,114,115]</sup>

To mitigate the structural design issues associated with nitrogen, oxygen or sulfur could also be used to introduce additional oxidation processes into the material. However, these heteroatoms tend to increase the redox potential of the resulting





**Scheme 2.** Structures of 5,10-dimethyl-5,10-dihydrophenazine (DHP-Me<sub>2</sub>) and 4,4'-dimethylviologen (Viologen-Me<sub>2</sub>) as examples of p-type RAGs undergoing a stable double oxidation, including molecular weight and theoretical specific capacity as well as their respective redox processes. Note that Viologen-Me<sub>2</sub> is stable in ambient conditions as the dicationic salt.

RAGs to values outside the stability window of conventional carbonate-based electrolytes ( $>4.2 \text{ V}$ ),<sup>[97]</sup> and the dicationic forms are prone to nucleophilic attack due to their high reactivity. This has been observed with phenothiazine,<sup>[116]</sup> phenoxazine,<sup>[117]</sup> and thianthrene,<sup>[80]</sup> where the second oxidation is possible in solution-based measurements but inaccessible in battery electrodes with carbonate-based electrolytes. In such heteroaromatics, the second oxidation can be enabled by attaching additional FGs (i.e., in 3,7-dimethoxyphenothiazines<sup>[116]</sup>),<sup>[118–120]</sup> changing the electrolyte type,<sup>[121]</sup> electrolyte stability window,<sup>[122]</sup> or shifting the redox potential of the RAG by salt concentration.<sup>[123]</sup>

#### 4.2. Immobilization of Organic Electrode Materials in Battery Electrodes

The ideal redox-active material would exclusively consist of redox-active structural units, with no “dead weight” to reduce the gravimetric capacity. In most cases, however, the addition of “inactive” structural units has either enabled synthetic access in the first place or has shown other beneficial effects that can compensate for a tolerable loss in capacity. The insolubility of the OAM in the battery electrolyte is one of the most important such effects. It is important to note, however, that depending on their SOC the solubility of OAMs in polar solvents of organic electrolytes can drastically change. For example, while p-type (hetero)aromatic compounds, in their neutral form, generally exhibit moderate to poor solubility in the organic solvents used in their synthesis, they often become soluble in battery electrolytes as soon as they are positively charged.<sup>[77,124–126]</sup> A dissolution of the OAM can lead to irreversible loss of contact with the current collector or transfer through the separator to the opposite electrode, where the material either causes a “short circuit” in the system or decomposes. This leads to a permanent loss of capacity or even failure of the

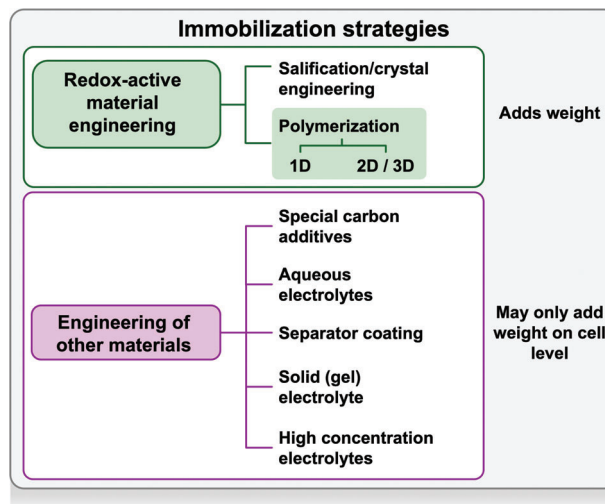


**Figure 14.** Overview and distinction of immobilization strategies to enhance the cycling lifetime of OAMs. Top: Strategies based on altering the chemical composition of the active material by synthetic design. Bottom: Strategies based on optimization of other components of the battery.

battery system.<sup>[127]</sup> Solubility in the electrolyte, or more specifically contact loss and crossover, are therefore some of the most important issues that have been tackled by researchers in recent years.<sup>[128–133]</sup>

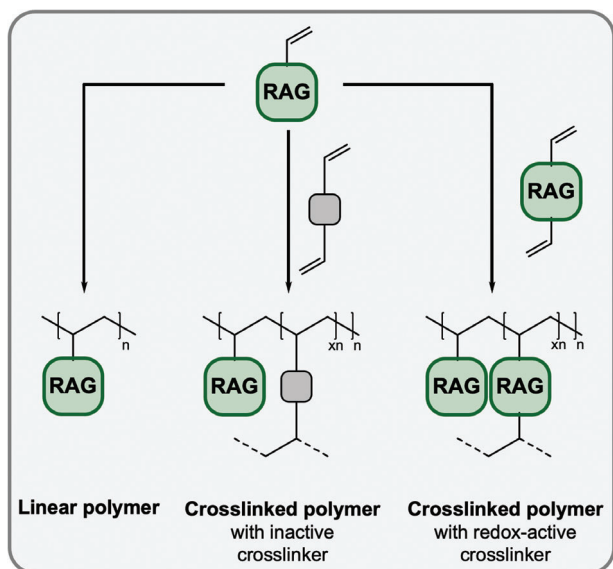
In general, the strategies for reducing the solubility of OAMs can be divided into those based on the synthetic production of the active material and those based on the modification of the “inactive” materials, e.g., the electrolyte and the separator, as shown in **Figure 14**.

There are numerous interesting approaches to suppressing solubility using the “inactive” materials of the battery cell. These include the simple screening of various solvents, but also more sophisticated approaches ranging from highly concentrated electrolytes,<sup>[134,135]</sup> solid-state electrolytes<sup>[102,122,136]</sup> and aqueous electrolyte systems<sup>[102,132,137–140]</sup> to special separator coatings/materials<sup>[133,141]</sup> and electrode carbon additives.<sup>[126,135,142–148]</sup> **Figure 14** provides a graphical overview of the various immobilization strategies.

This discussion will focus on strategies directly related to the synthetic engineering of the OAM (**Figure 14**, left), as they are part of the material design and therefore the responsibility of the synthetic chemist.

The most commonly used synthetic immobilization technique is polymer incorporation. Here, RAGs are incorporated into larger one- (linear polymers), two- (covalent organic frameworks (COFs)), or three-dimensional (cross-linked polymers or porous organic polymers (POPs)) structures or networks. Chain entanglement and/or the strengthening of other interactions between the chains, such as  $\pi$ -stacking, then leads to a drastic reduction in solubility.<sup>[102,149–153]</sup>

If the polymeric backbone enables conjugation between the RAGs, this can greatly improve the intramolecular electrical conductivity. Thus, the increase in molecular weight by the polymeric backbone can be alleviated by reducing the amount of conductive additive needed in the electrode mixture.<sup>[103,114,154–156]</sup>



**Scheme 3.** Principle of redox-active crosslinking agents for the example of a polymer created by radical polymerization. The dead weight added by crosslinking agents can be minimized if the RAG-monomer is equipped with two polymerizable groups and added as the crosslinker.

A second way to immobilize organic molecules is the so-called salification, i.e., the introduction of a salt in form of an ionic group, into the molecule.<sup>[130,157–163]</sup> The idea behind this approach is that the ionic substructures provide strong intermolecular interactions that facilitate the formation of crystalline or crystal-like structures that reduce solubility.<sup>[163]</sup> For this application, it is important that the potential redox activity of the ionic group lies outside the potential window of the application in question. The most common strategy for salification is the introduction of metal carboxylate groups into the molecule, pioneered by Armand et al. 2009.<sup>[83]</sup> In some cases, the stacking in small molecule crystals through intermolecular forces can be strong enough to suppress dissolution, even in the absence of ionic groups.<sup>[164]</sup>

Comparing the two methods, salting out by, i.e., adding a carboxylate group, leads to only a slight increase in molecular weight, but the immobilization effect is not as significant as with polymers and is also highly dependent on the electrolyte system. Polymerization, on the other hand, especially when done in a cross-linking fashion, adds the combined weight of backbone and crosslinker structures, resulting in a lower capacity. However, this is compensated for by the much stronger immobilization effect. The weight of the backbone and crosslinker can be reduced by using RAG-containing, electrochemically active variants of these structures, as shown in **Scheme 3**.

In summary, the applicability of advanced organic synthesis in the development of OAMs enables customized design of organic functional materials, which is one of their greatest advantages.

## 5. Applications for Organic Electrode Materials in Full-Cells

Organic batteries are still considered a new technology. In spite of the intensive research on OAMs of all conceivable polarities

and chemistries in the last decade,<sup>[39,106–109,111,128,156]</sup> the majority of reports still focus on fundamental research and the development of new materials with their characterization in half-cell batteries. In many cases, the focus still lies on the development of new materials, while optimization at the cell level is less frequently reported. Whether these materials are feasible for a full-cell and which type of full-cell is often not clear. Therefore, the much-advertised special properties and sustainability aspects of OAMs have yet to be harnessed for application, and there are few prototype applications.<sup>[165,166]</sup> Although interest in the optimization and eventual commercialization of organic batteries has increased in recent years, it still plays a subordinate role in research.<sup>[24,106,167]</sup> In this way, organic functional materials have not yet become as established in the battery world as in other areas such, as light-emitting diodes (OLED) or organic photovoltaics (OPV), where organic materials are a much more mature competitor to the respective conventional materials and have already been commercialized.<sup>[168–170]</sup>

The comparatively slow progress in organic energy storage and the lack of real applications can be attributed to several factors. One might think that the most obvious reason is that the technology is simply not advanced enough at this stage. However, there are some nuances to this problem. One of the main reasons for the lack of commercialization of organic batteries is certainly the sheer amount of active material needed for a real application. In OPV applications, the weight fraction of the organic active material in the final solar cell can be as little as 0.02%,<sup>[171]</sup> so even complicated organic molecules that require lengthy and expensive syntheses are still considered for application.<sup>[169]</sup> In batteries, on the other hand, the weight fraction of the active materials should be as high as possible compared to the electrochemically inactive parts in order to achieve the highest possible gravimetric capacity at the cell level. Consequently, the feasibility of large-scale material production is much more important for organic battery materials than for other applications of organic functional materials.

This is where the synthetic versatility of organic materials becomes one of their greatest challenges, as the synthetic toolbox of organic materials is mostly based on the stepwise assembly of structures. Thus, in more complicated synthetic routes, the embedded carbon and other unfavorable environmental impacts of organic synthesis<sup>[172]</sup> can exceed those of inorganic materials production,<sup>[173]</sup> which could effectively overcompensate for the sustainability aspects of organic pendants. Environmental impacts aside, many of the OAMs known to date are unsuitable for mass production simply due to their synthetic complexity.

The other rarely discussed problem facing organic batteries (in the same way as inorganic batteries) as a field of research is the low level of standardization in the generation and reporting of data.<sup>[174]</sup> Despite the large number of reports on different materials, many materials cannot be directly compared with each other because the cell and measurement parameters are not harmonized. Particularly in reports on full-cells, the performance data given are rarely truly comparable due to significantly different definitions or measurement methods. A definition of more performance metrics standards could alleviate this issue,<sup>[24,106,175]</sup> similar to what has been achieved for solar cells.

While the lack of standardization is a problem that needs to be addressed by the community outside the lab, the other

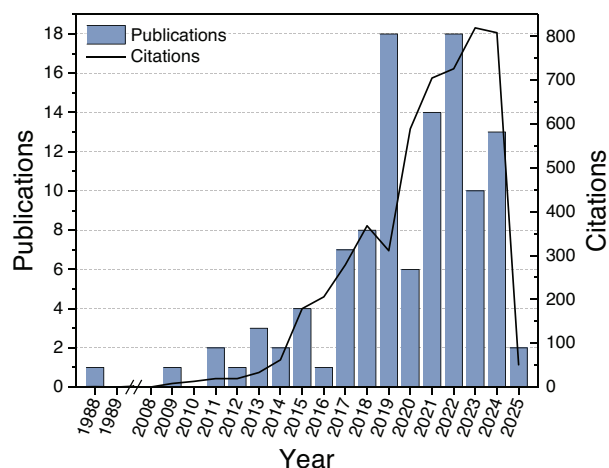


**Figure 15.** Number of publications per year containing “all-organic battery,” “full-organic battery,” or “totally organic battery” in the title (blue bars). Number of citations per year across all papers are shown as the black line. Data gathered from Web of Science in January 2025. Certain data included herein are derived from Clarivate (Web of Science). Clarivate 2025. All rights reserved.

shortcomings mentioned highlight the still prevalent immaturity of the research field. However, they also suggest that significant improvements could be possible in the future, provided that these problems are addressed by shifting research efforts to a more comprehensive approach.

OAMs are of high interest for so-called post-Li technologies (i.e., multivalent metal batteries), and great prospect also lies in their application in all-organic full-cells. Fortunately, there has been an increase in research interest and effort in all-organic battery cells in recent years, which may mark a turning point in the development curve of organic batteries (see Figure 8). This development can be illustrated by the number of publications containing “all-organic battery,” “full-organic battery,” or “totally organic battery” in the title and the corresponding citations in recent decades (Figure 15).

After Arnett et al.<sup>[177]</sup> reported the first case of a purely organic battery in 1988, there were no contributions in the field for just over 20 years until Suga et al. got the ball rolling again in 2009 with their report on a purely organic system of two different radical polymers.<sup>[178]</sup> Since then, the field has steadily grown, with a number of different cell chemistries emerging.

As explained above, there are generally two possible mechanisms for fully organic cell configurations. A dual-ion mechanism, in which both the cation and the anion perform a charge-transporting function (dual-ion cell), and the ion-rocking-chair mechanism (cation or anion-rocking-chair), in which only one of the two ionic species is active, while the other serves exclusively to balance the charge. In addition to this subdivision, the type of ions involved can also be varied. This applies in particular to the cation, which in conventional batteries is almost always a metal ion. However, there are reports showing that the metal ion can be replaced by organic molecular ions<sup>[178,179]</sup> or even protons,<sup>[137,180–183]</sup> potentially increasing sustainability even further, as lithium (and other metals) are completely removed from the system. In addition to the different charging mechanisms, an-

other important distinction is between batteries with organic or aqueous electrolytes. While aqueous electrolytes reduce the toxicity and flammability of the system, they are limited in voltage by the generation potential of hydrogen and oxygen. There is an entire field of research dedicated solely to optimizing this problem, whether for inorganic or organic active materials.<sup>[140,184]</sup>

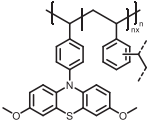
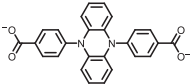
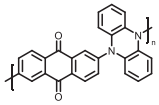
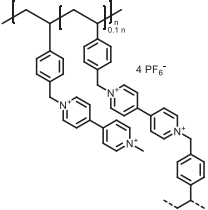
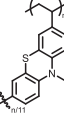
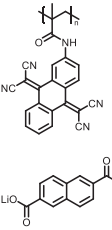
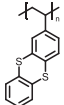
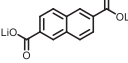
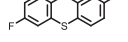
Poizot et al. provided a comprehensive review of literature reports on all-organic cells in 2018,<sup>[185]</sup> since then a number of publications have been added on dual-ion,<sup>[186,187]</sup> cation-rocking<sup>[183,188]</sup> and anion-rocking<sup>[71,115,189–191]</sup> chair cells. The latter attracted somewhat greater interest due to some desirable advantages of these systems, in which all transport is based solely on anion diffusion. Anions typically show faster diffusion,<sup>[192]</sup> and such batteries could be completely free of metals.

Until 2018, the focus of the field was primarily on so-called asymmetric cells, which consist of different positive and negative electrode materials. In asymmetric cells, virtually any two OAMs/EHCs can be combined which leaves room for countless combinations and careful fine-tuning of resulting performance parameters.

Symmetrical cells, on the other hand, are characterized by the fact that they only use a single material, which means that only one material needs to be synthesized and optimized. This can potentially save resources in development and production (as discussed before).<sup>[49,50]</sup> The first symmetrical all-organic batteries (SAOBs) were developed around the same time as the first organic semiconductors. These were based on the same principles as the first organic half-cells discussed above, which were based on charge storage by doping semiconducting polymers. This indicates that the concept of a symmetrical battery was already of interest in the 1980s,<sup>[55]</sup> the earliest example even coming from MACDIARMID and HEEGER<sup>[53]</sup> themselves. During the revival of the organic battery field in the late 2000s, the Porzot group was the first to also revive interest in SAOB cells by reporting the first such systems based on RAG electrochemistry<sup>[161]</sup> rather than the earlier doping-based approaches. This was followed by an increasing, but still single-digit, number of annual reports on dual-ion<sup>[91,94,162,181,191,193–198]</sup> and cation-rocking chair<sup>[27,182,199–208]</sup> SAOBs in recent years. Recently, we reported on the first all-organic symmetric anion-rocking chair battery using the cross-linked polymer poly(*N*-styryl-3,7-dimethoxy phenothiazine) (X-PSDMPT).<sup>[116]</sup> Of the two reversible oxidations of the phenothiazine units in this polymer, we used the first oxidation as the reaction at the negative electrode and the second oxidation as the positive electrode reaction.

To compare some of the most recent all-organic batteries Table 2 shows an overview of recent full-organic cells with the respective organic active materials. More detailed collections and comparisons of different (all-) organic batteries can be found in the literature.<sup>[106,185,209,210]</sup> In a techno-economic review article Innocenti et al. provide an overview of various n-type organic materials for lithium batteries and also compare the organic materials with their inorganic, commercially established counterparts NMC 622 and LFP (Lithium iron phosphate).<sup>[211]</sup> Additionally, they discuss the costs and energy density of the presented organic active materials. In their cost analysis, they name the often-complex synthetic routes and the costs per unit mass as main reasons why organic batteries are not necessarily more expensive than inorganic ones. As the organic materials are often

**Table 2.** Comparison of selected recent symmetric and asymmetric full-organic batteries, their organic active materials, and their characteristic parameters. NMC622 and LFP are shown as comparison to commercially established inorganic cathode active materials.

Negative electrode active material	Positive electrode active material	Specific capacity [mAh g <sup>-1</sup> ] (C-rate, if given)	Cell voltage [V]	Refs.
		61 (0.5 C)	0.55	[116]
		55 (1 C)	2.5	[162]
		125	0.7; 1.7	[198]
		65 (0.2 C)	0.9; 1.4	[71]
		105 (1 C)	1.35	[82]
		44 (0.2 C)	3.4	[186]
Graphite	NMC 622	174 (1 C)	3–4.4	[213]
Graphite	LFP	157 (1C)	3.4	[211]

lower in specific capacity and in energy density as higher quantity of active material is needed. Regarding the energy density assessment, Judez *et al.* provide a comprehensive analysis on energy densities auf various kinds of organic batteries.<sup>[212]</sup> In 2022, Zhang *et al.* published an article for a full life-cycle assessment of an all-organic battery with discussing also environmental issues. While they found the long synthetic routes and the associated large amounts of solvents that are used to have the greatest environmental impact, they also give suggestions on how to reduce these impacts during the synthesis of organic materials.<sup>[172]</sup>

## 6. Summary and Outlook

In summary, it can be said that great hopes lie in the development of market-ready organic (full-cell) battery systems. Progress in this field over the last decade has already unlocked some of the great potential of organic materials for energy storage. In the future, more and more focus will be placed on the remaining issues facing OAMs, such as a relatively low volumetric capacity and the embedded carbon footprint in the synthesis and produc-

tion of these materials. Research on organic electrode materials needs to focus on improving synthetic routes and costs per unit mass to increase the specific capacities and energy densities of the materials. This will hopefully pave the way toward real applications in the coming years. The application of organic-based energy storage materials will most likely impact non-conventional applications first, where their unique properties, such as ultra-fast charging, stretchability, processability in solution, etc., can give them the edge over inorganic materials.

Establishing research field-wide standards for measurement methods and reporting performance data are some of the first steps the community should take to facilitate and accelerate this process.

## Acknowledgements

This work contributes to the research performed at CELEST (Center for Electrochemical Energy Storage Ulm-Karlsruhe). It was funded by the German Research Foundation (DFG) under Project IDs 390874152 (POLiS Cluster of Excellence, EXC 2154) and 441236036 and by the European Union (ERC, NanOBatt, 101088146). Views and opinions expressed are



however those of the authors only and do not necessarily reflect those of the European Union or the European Research Council Executive Agency. Open access funding enabled and organized by Projekt DEAL.

## Conflict of Interest

The authors declare no conflict of interest.

## Keywords

energy storage, how-to, organic batteries, redox active, sustainability

Received: January 8, 2025

Revised: February 5, 2025

Published online: February 24, 2025

- [1] Trends in Batteries – Global EV Outlook 2023 – Analysis, <https://www.iea.org/reports/global-ev-outlook-2023/trends-in-batteries> (accessed: December 2024).
- [2] H. Zhang, C. Li, G. G. Eshetu, S. Laruelle, S. Grugeon, K. Zaghib, C. Julien, A. Mauger, D. Guyomard, T. Rojo, N. Gisbert-Trejo, S. Passerini, X. Huang, Z. Zhou, P. Johansson, M. Forsyth, *Angew. Chem.* **2020**, 132, 542.
- [3] M. Fichtner, K. Edström, E. Ayerbe, M. Berecibar, A. Bhowmik, I. E. Castelli, S. Clark, R. Dominko, M. Erakca, A. A. Franco, A. Grimaud, B. Horstmann, A. Latz, H. Lorrman, M. Meeus, R. Narayan, F. Pammer, J. Ruhland, H. Stein, T. Vegge, M. Weil, *Adv. Energy Mater.* **2022**, 12, 2102904.
- [4] Global Battery Market Size by Technology, <https://www.statista.com/statistics/1339880/global-battery-market-size-by-technology/> (accessed: December 2024).
- [5] Lithium Carbonate Price 2023, <https://www.statista.com/statistics/606350/battery-grade-lithium-carbonate-price/> (accessed: December 2024).
- [6] Nickel Price 1980–2023, <https://www.statista.com/statistics/236578/average-nickel-prices/> (accessed: December 2024).
- [7] Battery Price Per kWh 2023, <https://www.statista.com/statistics/883118/global-lithium-ion-battery-pack-costs/> (accessed: December 2024).
- [8] Lithium Global Supply Projection 2030, <https://www.statista.com/statistics/452026/projected-total-supply-for-lithium-globally/>, (accessed: December 2024).
- [9] Lithium Global Demand Forecast 2025, <https://www.statista.com/statistics/452025/projected-total-demand-for-lithium-globally/> (accessed: December 2024).
- [10] Global Nickel Reserves by Country 2023, <https://www.statista.com/statistics/273634/nickel-reserves-worldwide-by-country/> (accessed: December 2024).
- [11] Nickel Production by Leading Country 2023, <https://www.statista.com/statistics/264642/nickel-mine-production-by-country/> (accessed: December 2024).
- [12] Global Cobalt Production by Country 2023, <https://www.statista.com/statistics/264928/cobalt-mine-production-by-country/> (accessed: December 2024).
- [13] Global Cobalt Reserves by Country 2023, <https://www.statista.com/statistics/264930/global-cobalt-reserves/> (accessed: December 2024).
- [14] Europe: Supply of Raw Materials for Batteries 2030, <https://www.statista.com/statistics/1375159/supply-of-raw-materials-for-batteries-outlook-europe/> (accessed: December 2024).
- [15] B. Esser, H. Ehrenberg, M. Fichtner, A. Groß, J. Janek, *Adv. Energy Mater.* **2024**, 2402824.
- [16] M. Walter, M. V. Kovalenko, K. V. Kravchuk, *New J. Chem.* **2020**, 44, 1677.
- [17] J. W. Choi, D. Aurbach, *Nat. Rev. Mater.* **2016**, 1, 16013.
- [18] F. Duffner, N. Kronmeyer, J. Tübke, J. Leker, M. Winter, R. Schmuck, *Nat. Energy* **2021**, 6, 123.
- [19] S.-H. Chung, A. Manthiram, *Adv. Mater.* **2019**, 31, 1901125.
- [20] M. Salama, Rosy, R. A., R. Yemini, Y. Gofer, D. Aurbach, M. Noked, *ACS Energy Lett.* **2019**, 4, 436.
- [21] Y. Yang, H. Yang, X. Wang, Y. Bai, C. Wu, *J. Energy Chem.* **2022**, 64, 144.
- [22] Y. Chen, J. Xu, P. He, Y. Qiao, S. Guo, H. Yang, H. Zhou, *Sci. Bull.* **2022**, 67, 2449.
- [23] T. Li, M. Huang, X. Bai, Y.-X. Wang, *Prog. Nat. Sci. Mater. Int.* **2023**, 33, 151.
- [24] Y. Lu, J. Chen, *Nat. Rev. Chem.* **2020**, 4, 127.
- [25] J. Xiao, Y. Huang, Y. Ma, C. Li, L. Fu, W. Zeng, X. Wang, X. Li, M. Wang, B. Guo, Y. Lin, H. Cao, *Energy Storage Mater.* **2023**, 63, 103046.
- [26] M. D. Hager, B. Esser, X. Feng, W. Schuhmann, P. Theato, U. S. Schubert, *Adv. Mater.* **2020**, 32, 2000587.
- [27] N. Kim, S. Lienemann, Z. Khan, G. Greczynski, A. Rahmanudin, M. Vagin, F. Ahmed, I. Petsagkourakis, J. Edberg, X. Crispin, K. Tybrandt, *J. Mater. Chem. A* **2023**, 11, 25703.
- [28] C. Wang, T. He, J. Cheng, Q. Guan, B. Wang, *Adv. Funct. Mater.* **2020**, 30, 2004430.
- [29] B. Wang, H. Wang, W. Chen, P. Wu, L. Bu, L. Zhang, L. Wan, *J. Colloid Interface Sci.* **2020**, 572, 1.
- [30] K. Hatakeyama-Sato, H. Wakamatsu, K. Yamagishi, T. Fujie, S. Takeoka, K. Oyaizu, H. Nishide, *Small* **2019**, 15, 1805296.
- [31] A. Rahmanudin, Z. Khan, K. Tybrandt, N. Kim, *J. Mater. Chem. A* **2023**, 11, 22718.
- [32] S. Muench, R. Burges, A. Lex-Balducci, J. C. Brendel, M. Jäger, C. Friebe, A. Wild, U. S. Schubert, *J. Polym. Sci.* **2021**, 59, 494.
- [33] Z. Tehrani, T. Korochkina, S. Govindarajan, D. J. Thomas, J. O'Mahony, J. Kettle, T. C. Claypole, D. T. Gethin, *Org. Electron.* **2015**, 26, 386.
- [34] I. K. Ilic, V. Galli, L. Lamanna, P. Cataldi, L. Pasquale, V. F. Anness, A. Athanassiou, M. Caironi, *Adv. Mater.* **2023**, 35, 2211400.
- [35] R. D. Andrés, R. Wessling, J. Büttner, L. Pap, A. Fischer, B. Esser, U. Würfel, *Energy Environ. Sci.* **2023**, 16, 5255.
- [36] D.-Y. Han, C. K. Song, G. Lee, W.-J. Song, S. Park, *Adv. Mater. Technol.* **2024**, 9, 2302236.
- [37] Y. Liang, P. Zhang, J. Chen, *Chem. Sci.* **2013**, 4, 1330.
- [38] N. Goujon, N. Casado, N. Patil, R. Marcilla, D. Mecerreyes, *Prog. Polym. Sci.* **2021**, 122, 101449.
- [39] P. Poizot, J. Gaubicher, S. Renault, L. Dubois, Y. Liang, Y. Yao, *Chem. Rev.* **2020**, 120, 6490.
- [40] T.-T. Wu, G.-L. Dai, J.-J. Xu, F. Cao, X.-H. Zhang, Y. Zhao, Y.-M. Qian, *Rare Met.* **2023**, 42, 3269.
- [41] A. Jain, Y. Shin, K. A. Persson, *Nat. Rev. Mater.* **2016**, 1, 15004.
- [42] R. Gómez-Bombarelli, J. Aguilera-Iparraguirre, T. D. Hirzel, D. Duvenaud, D. Maclaurin, M. A. Blood-Forsythe, H. S. Chae, M. Einzinger, D.-G. Ha, T. Wu, G. Markopoulos, S. Jeon, H. Kang, H. Miyazaki, M. Numata, S. Kim, W. Huang, S. I. Hong, M. Baldo, R. P. Adams, A. Aspuru-Guzik, *Nat. Mater.* **2016**, 15, 1120.
- [43] A. F. de Almeida, R. Moreira, T. Rodrigues, *Nat. Rev. Chem.* **2019**, 3, 589.
- [44] C. López, *Adv. Mater.* **2023**, 35, 2208683.
- [45] G. Pilania, *Comput. Mater. Sci.* **2021**, 193, 110360.
- [46] R. P. Carvalho, C. F. N. Marchiori, D. Brandell, C. M. Araujo, *Energy Storage Mater.* **2022**, 44, 313.
- [47] R. Nölle, K. Beltrop, F. Holtstiege, J. Kasnatscheew, T. Placke, M. Winter, *Mater. Today* **2020**, 32, 131.



- [48] D. Doerffel, S. A. Sharkh, *J. Power Sources* **2006**, 155, 395.
- [49] H. Wang, C. Chen, C. Qian, C. Liang, Z. Lin, *RSC Adv.* **2017**, 7, 33273.
- [50] L. Zhang, S. X. Dou, H. K. Liu, Y. Huang, X. Hu, *Adv. Sci.* **2016**, 3, 1600115.
- [51] C. K. Morehouse, R. Glicksman, *J. Electrochem. Soc.* **1957**, 104, 467.
- [52] D. L. Williams, J. J. Byrne, J. S. Driscoll, *J. Electrochem. Soc.* **1969**, 116, 2.
- [53] D. MacInnes, M. A. Druy, P. J. Nigrey, D. P. Nairns, A. G. MacDiarmid, A. J. Heeger, *J. Chem. Soc. Chem. Commun.* **1981**, 7, 317.
- [54] L. W. Shacklette, R. L. Elsenbaumer, R. R. Chance, J. M. Sowa, D. M. Ivory, G. G. Miller, R. H. Baughman, *J. Chem. Soc. Chem. Commun.* **1982**, 6, 361.
- [55] K. Kaneto, K. Yoshino, Y. Inuishi, *Jpn. J. Appl. Phys.* **1983**, 22, L567.
- [56] T. Kobayashi, H. Yoneyama, H. Tamura, *J. Electroanal. Chem. Interfacial Electrochem.* **1984**, 177, 281.
- [57] A. G. MacDiarmid, L. S. Yang, W. S. Huang, B. D. Humphrey, *Synth. Met.* **1987**, 18, 393.
- [58] N. Mermilliod, J. Tanguy, F. Petiot, *J. Electrochem. Soc.* **1986**, 133, 1073.
- [59] Y. Liang, Y. Yao, *Joule* **2018**, 2, 1690.
- [60] K. Oyaizu, H. Nishide, *Adv. Mater.* **2009**, 21, 2339.
- [61] P. Passiniemi, J.-E. Österholm, *Synth. Met.* **1987**, 18, 637.
- [62] H. Alt, H. Binder, A. Köhling, G. Sandstedt, *Electrochim. Acta* **1972**, 17, 873.
- [63] M. Liu, S. J. Visco, L. C. D. Jonghe, *J. Electrochem. Soc.* **1989**, 136, 2570.
- [64] M. Liu, S. J. Visco, L. C. D. Jonghe, *J. Electrochem. Soc.* **1991**, 138, 1891.
- [65] O. Dedehayir, M. Steinert, *Technol. Forecast. Soc. Change* **2016**, 108, 28.
- [66] M. E. Speer, C. Sterzenbach, B. Esser, *ChemPlusChem* **2017**, 82, 1274.
- [67] G. Desmaizieres, M. E. Speer, I. Thiede, P. Gaiser, V. Perner, M. Kolek, P. Bieker, M. Winter, B. Esser, *Macromol. Rapid Commun.* **2021**, 42, 2000725.
- [68] J. Sprachmann, T. Wachsmuth, M. Bhosale, D. Burmeister, G. J. Smales, M. Schmidt, Z. Kochovski, N. Grabicki, R. Wessling, E. J. W. List-Kratochvil, B. Esser, O. Dumele, *J. Am. Chem. Soc.* **2023**, 145, 2840.
- [69] K. Deuchert, S. Hünig, *Angew. Chem. Int. Ed. Engl.* **1978**, 17, 875.
- [70] Z. X. Chen, Y. Li, F. Huang, *Chem* **2021**, 7, 288.
- [71] M. Bhosale, C. Schmidt, P. Penert, G. Studer, B. Esser, *ChemSusChem* **2024**, 17, 202301143.
- [72] A. Yu, C. Li, X. Chen, C. Zhang, S. Mei, C.-J. Yao, *ChemSusChem* **2024**, 17, 202301809.
- [73] G. Dai, X. Wang, Y. Qian, Z. Niu, X. Zhu, J. Ye, Y. Zhao, X. Zhang, *Energy Storage Mater.* **2019**, 16, 236.
- [74] L. Xu, Q. Fei, L. Yao, C. Su, *J. Mater. Chem. A* **2024**, 12, 13320.
- [75] M. Guo, W. Li, W. Tang, C. Tang, B. Cao, X. He, C. Fan, *Energy Storage Mater.* **2025**, 74, 103979.
- [76] J. Guo, X. Peng, B. Ouyang, D. Huang, Z. Jing, X. Bian, Y. Du, H. Yang, *New J. Chem.* **2024**, 48, 11211.
- [77] M. Kolek, F. Otteny, P. Schmidt, C. Mück-Lichtenfeld, C. Einholz, J. Becking, E. Schleicher, M. Winter, P. Bieker, B. Esser, *Energy Environ. Sci.* **2017**, 10, 2334.
- [78] S. Zhang, J. Cai, H. Li, F. Xing, L. Chen, X. Wang, X. He, *Adv. Energy Mater.* **2025**, 15, 2403029.
- [79] T. Wu, Y. Liu, J. Ye, Y. Chen, G. Dai, X. Zhang, Y. Zhao, *J. Power Sources* **2024**, 612, 234779.
- [80] M. E. Speer, M. Kolek, J. J. Jassoy, J. Heine, M. Winter, P. M. Bieker, B. Esser, *Chem. Commun.* **2015**, 51, 15261.
- [81] A. Basit, M. G. Mohamed, S. U. Sharma, S.-W. Kuo, *ACS Appl. Polym. Mater.* **2024**, 6, 12247.
- [82] A. Wild, M. Strumpf, B. Häupler, M. D. Hager, U. S. Schubert, *Adv. Energy Mater.* **2017**, 7, 1601415.
- [83] M. Armand, S. Grugeon, H. Vezin, S. Laruelle, P. Ribière, P. Poizot, J.-M. Tarascon, *Nat. Mater.* **2009**, 8, 120.
- [84] A. J. Bard, L. R. Faulkner, *Electrochemical Methods: Fundamentals and Applications*, Wiley, New York, **2001**.
- [85] H. Wu, K. Wang, Y. Meng, K. Lu, Z. Wei, *J. Mater. Chem. A* **2013**, 1, 6366.
- [86] J. Brown, M. Karlsmo, E. Bendadesse, P. Johansson, A. Grimaud, *Energy Storage Mater.* **2024**, 66, 103218.
- [87] B. Tian, Z. Ding, G.-H. Ning, W. Tang, C. Peng, B. Liu, J. Su, C. Su, K. P. Loh, *Chem. Commun.* **2017**, 53, 2914.
- [88] R. Grieco, O. Luzanin, D. Alvan, M. Liras, R. Dominko, N. Patil, J. Bitenc, R. Marcilla, *Faraday Discuss.* **2024**, 250, 110.
- [89] J. Xie, W. Chen, G. Long, W. Gao, Z. J. Xu, M. Liu, Q. Zhang, *J. Mater. Chem. A* **2018**, 6, 12985.
- [90] W. Guo, Y.-X. Yin, S. Xin, Y.-G. Guo, L.-J. Wan, *Energy Environ. Sci.* **2012**, 5, 5221.
- [91] G. Son, V. Ri, D. Shin, Y. Jung, C. B. Park, C. Kim, *Adv. Sci.* **2023**, 10, 2301993.
- [92] J. J. Heo, J. Ryu, *Korean J. Chem. Eng.* **2024**, <https://link.springer.com/article/10.1007/s11814-024-00255-6#citeas>
- [93] H. Wang, Y. Wang, Q. Wu, G. Zhu, *Mater. Today* **2022**, 52, 269.
- [94] T. Suga, S. Sugita, H. Ohshiro, K. Oyaizu, H. Nishide, *Adv. Mater.* **2011**, 23, 751.
- [95] P. Gerlach, R. Burges, A. Lex-Balducci, U. S. Schubert, A. Balducci, *Electrochim. Acta* **2019**, 306, 610.
- [96] J. Qin, Q. Lan, N. Liu, F. Men, X. Wang, Z. Song, H. Zhan, *iScience* **2019**, 15, 16.
- [97] J. Alvarado, M. A. Schroeder, M. Zhang, O. Borodin, E. Gobrogge, M. Olguin, M. S. Ding, M. Gobet, S. Greenbaum, Y. S. Meng, K. Xu, *Mater. Today* **2018**, 21, 341.
- [98] A. Ramasubramanian, V. Yurkiv, T. Foroozan, M. Ragone, R. Shahbazian-Yassar, F. Mashayek, *J. Phys. Chem. C* **2019**, 123, 10237.
- [99] W. Liu, P. Liu, D. Mitlin, *Adv. Energy Mater.* **2020**, 10, 2002297.
- [100] N. von Aspern, G.-V. Rösenthaler, M. Winter, I. Kekić-Laskovic, *Angew. Chem., Int. Ed.* **2019**, 58, 15978.
- [101] R. Raccichini, M. Amores, G. Hinds, *Batteries* **2019**, 5, 12.
- [102] M. Li, R. P. Hicks, Z. Chen, C. Luo, J. Guo, C. Wang, Y. Xu, *Chem. Rev.* **2023**, 123, 1712.
- [103] P. Acker, J. S. Wössner, G. Desmaizieres, B. Esser, A. C. S. Sustain, *Chem. Eng.* **2022**, 10, 3236.
- [104] S. Hillebrandt, T. Adermann, M. Alt, J. Schinke, T. Glaser, E. Mankel, G. Hernandez-Sosa, W. Jaegermann, U. Lemmer, A. Pucci, W. Kowalsky, K. Müllen, R. Lovrincic, M. Hamburger, *ACS Appl. Mater. Interfaces* **2016**, 8, 4940.
- [105] S. R. Peurifoy, J. C. Russell, T. J. Sisto, Y. Yang, X. Roy, C. Nuckolls, *J. Am. Chem. Soc.* **2018**, 140, 10960.
- [106] J. Kim, Y. Kim, J. Yoo, G. Kwon, Y. Ko, K. Kang, *Nat. Rev. Mater.* **2023**, 8, 54.
- [107] H. Wang, C.-J. Yao, H.-J. Nie, K.-Z. Wang, Y.-W. Zhong, P. Chen, S. Mei, Q. Zhang, *J. Mater. Chem. A* **2020**, 8, 11906.
- [108] J. Xie, Q. Zhang, *Small* **2019**, 15, 1805061.
- [109] B. Esser, *Org. Mater.* **2019**, 1, 63.
- [110] H. Chen, M. Armand, G. Demailly, F. Dolhem, P. Poizot, J.-M. Tarascon, *ChemSusChem* **2008**, 1, 348.
- [111] H. Kye, Y. Kang, D. Jang, J. E. Kwon, B.-G. Kim, *Adv. Energy Sustain. Res.* **2022**, 3, 2200030.
- [112] H. Dong, N. Kang, L. Li, L. Li, Y. Yu, S. Chou, *Adv. Mater.* **2024**, 36, 2311401.
- [113] P. Acker, M. E. Speer, J. S. Wössner, B. Esser, *J. Mater. Chem. A* **2020**, 8, 11195.

- [114] X. Zhao, X. Qiu, H. Xue, S. Liu, D. Liang, C. Yan, W. Chen, Y. Wang, G. Zhou, *Angew. Chem.* **2023**, 135, e202216713.
- [115] V. Cadiou, A.-C. Gaillot, É. Deunf, F. Dolhem, L. Dubois, T. Gutel, P. Poizot, *ChemSusChem* **2020**, 13, 2345.
- [116] R. Wessling, H. Koger, F. Otteny, M. Schmidt, A. Semmelmaier, B. Esser, *ACS Appl. Polym. Mater.* **2024**, 6, 7956.
- [117] F. Otteny, V. Perner, D. Wassy, M. Kolek, P. Bieker, M. Winter, B. Esser, *ACS Sustain. Chem. Eng.* **2020**, 8, 238.
- [118] J. A. Kowalski, M. D. Casselman, A. P. Kaur, J. D. Milshtein, C. F. Elliott, S. Modekrutti, N. H. Attanayake, N. Zhang, S. R. Parkin, C. Risko, F. R. Brushett, S. A. Odom, *J. Mater. Chem. A* **2017**, 5, 24371.
- [119] F. Zhang, Y. Cheng, Z. Niu, J. Ye, G. Dai, X. Zhang, Y. Zhao, *Chem-ElectroChem* **2020**, 7, 1781.
- [120] K. M. Pelzer, L. Cheng, L. A. Curtiss, *J. Phys. Chem. C* **2017**, 121, 237.
- [121] G. Studer, A. Schmidt, J. Büttner, M. Schmidt, A. Fischer, I. Krossing, B. Esser, *Energy Environ. Sci.* **2023**, 16, 3760.
- [122] Y. Zheng, H. Ji, J. Liu, Z. Wang, J. Zhou, T. Qian, C. Yan, *Nano Lett.* **2022**, 22, 3473.
- [123] S. Lee, K. Lee, K. Ku, J. Hong, S. Y. Park, J. E. Kwon, K. Kang, *Adv. Energy Mater.* **2020**, 10, 2001635.
- [124] F. Otteny, M. Kolek, J. Becking, M. Winter, P. Bieker, B. Esser, *Adv. Energy Mater.* **2018**, 8, 1802151.
- [125] V. Perner, D. Diddens, F. Otteny, V. Küpers, P. Bieker, B. Esser, M. Winter, M. Kolek, *ACS Appl. Mater. Interfaces* **2021**, 13, 12442.
- [126] B. Tengen, T. Winkelmann, N. Ortlieb, V. Perner, G. Studer, M. Winter, B. Esser, A. Fischer, P. Bieker, *Adv. Funct. Mater.* **2023**, 33, 2210512.
- [127] V. W. Lau, I. Moudrakovski, J. Yang, J. Zhang, Y.-M. Kang, *Angew. Chem.* **2020**, 132, 4052.
- [128] B. Häupler, A. Wild, U. S. Schubert, *Adv. Energy Mater.* **2015**, 5, 1402034.
- [129] Y. Liu, Z. Niu, G. Dai, Y. Chen, H. Li, L. Huang, X. Zhang, Y. Xu, Y. Zhao, *Mater. Today Energy* **2021**, 21, 100812.
- [130] P. Poizot, F. Dolhem, *Energy Environ. Sci.* **2011**, 4, 2003.
- [131] M. Kolek, F. Otteny, J. Becking, M. Winter, B. Esser, P. Bieker, *Chem. Mater.* **2018**, 30, 6307.
- [132] Y. Liang, Y. Jing, S. Gheyhani, K.-Y. Lee, P. Liu, A. Facchetti, Y. Yao, *Nat. Mater.* **2017**, 16, 841.
- [133] H. Dong, O. Tutusaus, Y. Liang, Y. Zhang, Z. Lebens-Higgins, W. Yang, R. Mohtadi, Y. Yao, *Nat. Energy* **2020**, 5, 1043.
- [134] T. Cai, Y. Han, Q. Lan, F. Wang, J. Chu, H. Zhan, Z. Song, *Energy Storage Mater.* **2020**, 31, 318.
- [135] Md. Adil, M. Schmidt, J. Vogt, T. Diemant, M. Oschatz, B. Esser, *Batter. Supercaps* **2024**, 7, e202400312.
- [136] X. Chi, F. Hao, J. Zhang, X. Wu, Y. Zhang, S. Gheyhani, Z. Wen, Y. Yao, *Nano Energy* **2019**, 62, 718.
- [137] C. Strietzel, M. Sterby, H. Huang, M. Strømme, R. Emanuelsson, M. Sjödin, *Angew. Chem., Int. Ed.* **2020**, 59, 9631.
- [138] C. Dong, F. Xu, L. Chen, Z. Chen, Y. Cao, *Small Struct.* **2021**, 2, 2100001.
- [139] H. Kim, J. Hong, K.-Y. Park, H. Kim, S.-W. Kim, K. Kang, *Chem. Rev.* **2014**, 114, 11788.
- [140] J. Xie, Z. Liang, Y.-C. Lu, *Nat. Mater.* **2020**, 19, 1006.
- [141] R. L. Belanger, B. Commarié, A. Paoletta, J.-C. Daigle, S. Bessette, A. Vijh, J. P. Claverie, K. Zaghib, *Sci. Rep.* **2019**, 9, 1213.
- [142] R. Shi, L. Liu, Y. Lu, Y. Li, S. Zheng, Z. Yan, K. Zhang, J. Chen, *Adv. Energy Mater.* **2021**, 11, 2002917.
- [143] K. Amin, Q. Meng, A. Ahmad, M. Cheng, M. Zhang, L. Mao, K. Lu, Z. Wei, *Adv. Mater.* **2018**, 30, 1703868.
- [144] S. Zhang, S. Ren, D. Han, M. Xiao, S. Wang, L. Sun, Y. Meng, *ACS Appl. Mater. Interfaces* **2020**, 12, 36237.
- [145] Z. Zhu, J. Chen, *J. Electrochem. Soc.* **2015**, 162, A2393.
- [146] K. Pirnat, R. Dominko, R. Cerc-Korosec, G. Mali, B. Genorio, M. Gaberscek, *J. Power Sources* **2012**, 199, 308.
- [147] B. Genorio, K. Pirnat, R. Cerc-Korosec, R. Dominko, M. Gaberscek, *Angew. Chem. Int. Ed.* **2010**, 49, 7222.
- [148] C. Tang, B. Wei, W. Tang, Y. Hong, M. Guo, X. He, J. Hu, S. Jia, C. Fan, *Chem. Eng. J.* **2023**, 474, 145114.
- [149] F. Otteny, G. Desmaizieres, B. Esser, *Redox Polymers for Energy and Nanomedicine*, The Royal Society of Chemistry, London **2020**, pp. 166-197.
- [150] E. Grignon, A. M. Battaglia, J. T. Liu, B. T. McAllister, D. S. Seferos, *ACS Appl. Mater. Interfaces* **2023**, 15, 45345.
- [151] F. Otteny, V. Perner, C. Einholz, G. Desmaizieres, E. Schleicher, M. Kolek, P. Bieker, M. Winter, B. Esser, *ACS Appl. Energy Mater.* **2021**, 4, 7622.
- [152] J. Hou, H. Liu, M. Gao, Q. Pan, Y. Zhao, *Angew. Chem., Int. Ed.* **2025**, 64, e202414566.
- [153] R. Dantas, C. Ribeiro, M. Souto, *Chem. Commun.* **2023**, 60, 138.
- [154] P. Acker, L. Rzesny, C. F. N. Marchiori, C. M. Araujo, B. Esser, *Adv. Funct. Mater.* **2019**, 29, 1906436.
- [155] Q. Yuan, C. Li, X. Guo, J. Zhao, Y. Zhang, B. Wang, Y. Dong, L. Liu, *Energy Rep* **2020**, 6, 2094.
- [156] S. Muench, A. Wild, C. Friebe, B. Häupler, T. Janoschka, U. S. Schubert, *Chem. Rev.* **2016**, 116, 9438.
- [157] A. Jouhara, L. Rzesny, V. Rialland, C. Latouche, P. Poizot, B. Esser, *ChemSusChem* **2023**, 16, 202300286.
- [158] S. Gottis, A.-L. Barrès, F. Dolhem, P. Poizot, *ACS Appl. Mater. Interfaces* **2014**, 6, 10870.
- [159] C. Wang, Y. Xu, Y. Fang, M. Zhou, L. Liang, S. Singh, H. Zhao, A. Schober, Y. Lei, *J. Am. Chem. Soc.* **2015**, 137, 3124.
- [160] Y. Hua, Y. Huang, Y. Wang, Y. Du, H. Yang, *New J. Chem.* **2021**, 45, 21534.
- [161] H. Chen, M. Armand, M. Courty, M. Jiang, C. P. Grey, F. Dolhem, J.-M. Tarascon, P. Poizot, *J. Am. Chem. Soc.* **2009**, 131, 8984.
- [162] G. Dai, Y. He, Z. Niu, P. He, C. Zhang, Y. Zhao, X. Zhang, H. Zhou, *Angew. Chem. Int. Ed.* **2019**, 58, 9902.
- [163] A. Shimizu, H. Kuramoto, Y. Tsujii, T. Nokami, Y. Inatomi, N. Hojo, H. Suzuki, J. Yoshida, *J. Power Sources* **2014**, 260, 211.
- [164] T. Chen, H. Banda, J. Wang, J. J. Oppenheim, A. Franceschi, M. Dincă, *ACS Cent. Sci.* **2024**, 10, 569.
- [165] M.-B. Group, Mercedes-Benz VISION AVTR, <https://group.mercedes-benz.com/innovation/product-innovation/design/vision-avtr-bci.html> (accessed: December 2024).
- [166] World Premiere: CMBlu Delivers First Organic SolidFlow Battery to One of the Biggest Solar Parks in Austria, <https://www.cmblu.com/en/press-and-media/first-solidflow-energy-storage-system-delivered/> (accessed: December 2024).
- [167] H. Zhang, Y. Gao, X.-H. Liu, Z. Yang, X.-X. He, L. Li, Y. Qiao, W.-H. Chen, R.-H. Zeng, Y. Wang, S.-L. Chou, *Adv. Funct. Mater.* **2022**, 32, 2107718.
- [168] A. Anctil, M. N. Beattie, C. Case, A. Chaudhary, B. D. Chrysler, M. G. Debié, S. Essig, D. K. Ferry, V. E. Ferry, M. Freitag, I. Gould, K. Hinzer, H. Hoppe, O. Inganäs, L. K. Jagadamma, M. H. Jee, R. K. Kostuk, D. Kirk, S. Kube, M. Lim, J. M. Luther, L. Mansfield, M. D. McGehee, D. N. Minh, P. Nain, M. O. Reese, A. Reinders, I. D. W. Samuel, W. van Sark, H. Savin, et al., *J. Photonics Energy* **2023**, 13, 042301.
- [169] I. McCulloch, M. Chabiny, C. Brabec, C. B. Nielsen, S. E. Watkins, *Nat. Mater.* **2023**, 22, 1304.
- [170] J. Panidi, D. G. Georgiadou, T. Schoetz, T. Prodromakis, *Adv. Funct. Mater.* **2022**, 32, 2200694.
- [171] Heliatic GmbH.
- [172] S. Zhang, N. Ericsson, P.-A. Hansson, M. Sjödin, Å. Nordberg, *J. Clean. Prod.* **2022**, 337, 130454.
- [173] M. Gutsch, J. Leker, *Appl. Energy* **2024**, 353, 122132.
- [174] N. M. Vargas-Barbosa, *Nat. Nanotechnol.* **2024**, 19, 419.

- [175] J. Bitenc, K. Pirnat, O. Lužanin, R. Dominko, *Chem. Mater.* **2024**, 36, 1025.
- [176] T. Song, D. J. Friedman, N. Kopidakis, *Adv. Energy Mater.* **2021**, 11, 2100728.
- [177] E. M. Arnett, L. G. Whitesell, J.-P. Cheng, E. Marchot, *Tetrahedron Lett.* **1988**, 29, 1507.
- [178] T. Suga, H. Ohshiro, S. Ugita, K. Oyaizu, H. Nishide, *Adv. Mater.* **2009**, 21, 1627.
- [179] M. Yao, H. Sano, H. Ando, T. Kiyobayashi, *Sci. Rep.* **2015**, 5, 10962.
- [180] R. Emanuelsson, M. Sterby, M. Strømme, M. Sjödin, *J. Am. Chem. Soc.* **2017**, 139, 4828.
- [181] T. Sun, H. Du, S. Zheng, J. Shi, X. Yuan, L. Li, Z. Tao, *Small Methods* **2021**, 5, 2100367.
- [182] Z. Tie, S. Deng, H. Cao, M. Yao, Z. Niu, J. Chen, *Angew. Chem., Int. Ed.* **2022**, 61, e202115180.
- [183] H. Wang, R. Emanuelsson, C. Karlsson, P. Jannasch, M. Strømme, M. Sjödin, *ACS Appl. Mater. Interfaces* **2021**, 13, 19099.
- [184] C. Liu, X. Chi, Q. Han, Y. Liu, *Adv. Energy Mater.* **2020**, 10, 1903589.
- [185] P. Poizot, F. Dolhem, J. Gaubicher, *Curr. Opin. Electrochem.* **2018**, 9, 70.
- [186] R. Russo, J.-N. Chotard, G. Gachot, C. Frayret, G. Toussaint, P. Stevens, M. Becuwe, *ACS Energy Lett.* **2023**, 8, 4597.
- [187] S. Jiang, W. Li, Y. Xie, X. Yan, K. Zhang, Z. Jia, *Chem. Eng. J.* **2022**, 434, 134651.
- [188] X. Wang, W. Tang, Y. Hu, W. Liu, Y. Yan, L. Xu, C. Fan, *Green Chem.* **2021**, 23, 6090.
- [189] A. Jouhara, E. Quarez, F. Dolhem, M. Armand, N. Dupré, P. Poizot, *Angew. Chem* **2019**, 131, 15827.
- [190] T. P. Nguyen, A. D. Easley, N. Kang, S. Khan, S.-M. Lim, Y. H. Rezenom, S. Wang, D. K. Tran, J. Fan, R. A. Letteri, X. He, L. Su, C.-H. Yu, J. L. Lutkenhaus, K. L. Wooley, *Nature* **2021**, 593, 61.
- [191] M. Uhl, Sadeeda, P. P., P. A. Schuster, B. W. Schick, S. Muench, A. Farkas, U. S. Schubert, B. Esser, A. J. C. Kuehne, T. Jacob, *ChemSusChem* **2024**, 17, 202301057.
- [192] K. Hayamizu, *J. Chem. Eng. Data* **2012**, 57, 2012.
- [193] H. Wang, H. Wang, Z. Si, Q. Li, Q. Wu, Q. Shao, L. Wu, Y. Liu, Y. Wang, S. Song, H. Zhang, *Angew. Chem* **2019**, 131, 10310.
- [194] P. Leung, J. Bu, P. Q. Velasco, M. R. Roberts, N. Grobert, P. S. Grant, *Adv. Energy Mater.* **2019**, 9, 1901418.
- [195] N. Casado, D. Mantione, D. Shanmukaraj, D. Mecerreyes, *ChemSusChem* **2020**, 13, 2464.
- [196] J. Kim, H. Kim, S. Lee, G. Kwon, T. Kang, H. Park, O. Tamwattana, Y. Ko, D. Lee, K. Kang, *J. Mater. Chem. A* **2021**, 9, 14485.
- [197] J. Wang, H. Liu, C. Du, Y. Liu, B. Liu, H. Guan, S. Guan, Z. Sun, H. Yao, *Chem. Sci.* **2022**, 13, 11614.
- [198] B. Wei, Y. Hong, W. Tang, M. Guo, X. He, C. Tang, J. Hu, C. Fan, *Chem. Eng. J.* **2023**, 451, 138773.
- [199] S. Wang, L. Wang, K. Zhang, Z. Zhu, Z. Tao, J. Chen, *Nano Lett.* **2013**, 13, 4404.
- [200] S. Wang, L. Wang, Z. Zhu, Z. Hu, Q. Zhao, J. Chen, *Angew. Chem., Int. Ed.* **2014**, 53, 5892.
- [201] Q. Zhao, J. Wang, Y. Lu, Y. Li, G. Liang, J. Chen, *Angew. Chem., Int. Ed.* **2016**, 55, 12528.
- [202] X. Chi, Y. Liang, F. Hao, Y. Zhang, J. Whiteley, H. Dong, P. Hu, S. Lee, Y. Yao, *Angew. Chem., Int. Ed.* **2018**, 57, 2630.
- [203] A. Jouhara, N. Dupré, A.-C. Gaillot, D. Guyomard, F. Dolhem, P. Poizot, *Nat. Commun.* **2018**, 9, 4401.
- [204] J. Xie, Z. Wang, Z. J. Xu, Q. Zhang, *Adv. Energy Mater.* **2018**, 8, 1703509.
- [205] K. Li, J. Yu, Z. Si, B. Gao, H. Wang, Y. Wang, *Chem. Eng. J.* **2022**, 450, 138052.
- [206] Z. Li, Q. Jia, Y. Chen, K. Fan, C. Zhang, G. Zhang, M. Xu, M. Mao, J. Ma, W. Hu, C. Wang, *Angew. Chem., Int. Ed.* **2022**, 61, e202207221.
- [207] S. Xu, C. Wang, T. Song, H. Yao, J. Yang, X. Wang, J. Zhu, C.-S. Lee, Q. Zhang, *Adv. Sci.* **2023**, 10, 2304497.
- [208] C. Liang, X. Cai, J. Lin, Y. Chen, Y. Xie, Y. Liu, *ChemPlusChem* **2024**, 89, 202300620.
- [209] H. Guo, H. Dai, C. Wang, *ChemPlusChem* **2023**, 88, 202300026.
- [210] Z. Yu, Y. Wang, Z. Luo, *Ind. Eng. Chem. Res.* **2024**, 63, 9619.
- [211] A. Innocenti, H. Adenusi, S. Passerini, *InfoMat* **2023**, 5, e12480.
- [212] X. Judez, L. Qiao, M. Armand, H. Zhang, *ACS Appl. Energy Mater.* **2019**, 2, 4008.
- [213] R. Jung, P. Strobl, F. Maglia, C. Stinner, H. A. Gasteiger, *J. Electrochem. Soc.* **2018**, 165, A2869.



**Robin Wessling** is a postdoctoral researcher at the Technical University of Denmark (DTU). His Master's and PhD theses in the group of Prof. Dr. Birgit Esser were focused on the synthesis and application of redox-active organic polymers for the development of organic photo-batteries and all-organic batteries. He obtained his PhD in 2024 at Ulm University, Germany.



**Philipp Penert** is a doctoral researcher in the group of Prof. Dr. Birgit Esser at Ulm University, Germany. He obtained his Bachelor's and Master's degrees at the University of Heidelberg, Germany, and joined the Esser group in 2021. He is working on the synthesis of redox-active polymers for organic batteries as well as on the fabrication of all-organic battery cells.



**Birgit Esser** is a Full Professor of Organic Chemistry at Ulm University, Germany. She obtained her Ph.D. in 2008 at the University of Heidelberg, Germany. After postdoctoral studies at the Massachusetts Institute of Technology as Leopoldina fellow from 2009 to 2012, she joined the University of Bonn, Germany, as Liebig and later Emmy-Noether junior group leader. From 2015 to 2021 she was Associate Professor for Molecular/Organic Functional Materials at the University of Freiburg, Germany, before joining Ulm University in 2022. Her research focuses on organic electrode materials for post-Li batteries, hoop-shaped, conjugated  $\pi$ -systems, and photo(redox) catalysis.